# Techniques

1906 Breast Tissue Imaging with Light Coherence Tomography: A Pilot Study.
O Assayag, A Burcheri, M Antoine, B Sigal, C Boccara. ESPCI ParisTech, France; Tenon Hospital, Paris, France; Curie Institute, Paris, France; LLTech, Paris, France.
Background: Breast cancer is the most common cancer and the second leading cause of death for women in western countries. Despite advances in early detection, breast imaging, and increased diagnosis of small tumors (cT1), up to 36% of breast-conserving surgery patients require subsequent excisions to achieve disease-free margins. The peroperatory evaluation of margins during surgery is time consuming, and the research for new techniques is justified. This pilot study aims to evaluate Light Coherence Tomography (Light-CT) as a tool for optical biopsies and imaging of benign and malignant human breast tissues.
Design: A Light CT scanner based on Full Field Optical Coherence Tomography (FFOCT) has been used to image human breast tissues. The light CT scanner has a<2μm axial resolution and <2μm transverse resolution. 40 breast specimens have been imaged from at least 10 different patients covering healthy tissues from post and pre-menopausic women, lobular and ductal carcinoma, and sentinel nodes, after or without fixation. The time required and safety of a Light-CT imaging procedure have also been evaluated.
Results: Good structural correspondence is observed between Light-CT images and histological sections.
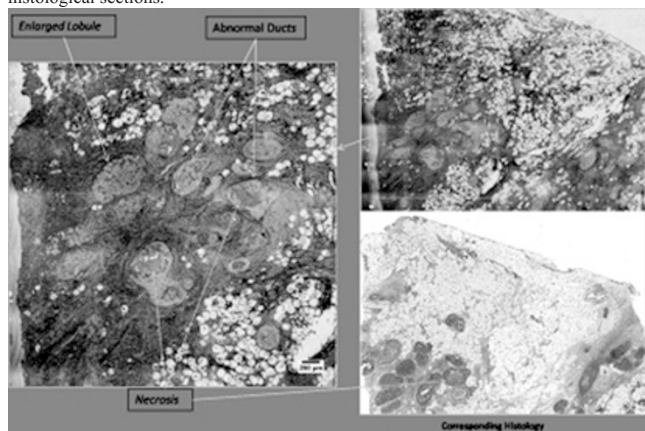
Characteristic features such as ducts, lobules, vessels, adipous, fibrous and necrotic tissue can be identified from Light-CT images and are recognized on normal and malignant tissue. Morphometric data such as the size of lobules and ducts and thickness of the parietal wall of the ducts and vessels as characteristics of these structures related to the presence of elastic tissue, can provide an additional diagnostic information. 9x9mm Light-CT images have been obtained in 2,5 minutes. Light-CT technology is safe since histology has been possible on 100% of the breast tissue samples.
Conclusions: We have demonstrated that the light CT technology is a fast and safe tool that can be used under clinical conditions. The Light CT images allow to recognize breast tissue structures and pathologies by comparison with traditional histology.

1907 Validation of Quantitative Real Time PCR for JAK2 Mutation Detection by Using $2^{-\Delta\Delta Ct}$ Method.
R Batra, C-K Huang, Q Pan. St Luke's Roosevelt Hospital Center, University Hospital of Columbia University College of Physicians and Surgeons, New York, NY; Montefiore Medical Center, Albert Einstein College of Medicine, New York, NY.
Background: The V617F mutation of the Janus kinase2 (JAK2) gene is a useful biomarker for the diagnosis of myeloproliferative disorders (MPD) such as polycythemia vera (PV), essential thrombocythemia (ET) and myeloid metaplasia with myelofibrosis (MF). JAK2 V617F is a gain of function mutation that leads to clonal proliferation; it is present in about 95% of PV cases and 50% of ET and MF cases. The aim of this study was to compare 2 methods for JAK2 mutation detection such as restriction fragment length polymorphism (RFLP) and real time PCR with $2^{-\Delta\Delta Ct}$ calculation.
Design: In a retrospective cohort study, 254 samples were analyzed for genomic DNA from blood or bone marrow with the RFLP assay and real time PCR. In RFLP, PCR is used to amplify the portion of JAK2 mutation bearing region. Amplicon products are then digested with the Bsa XI restriction enzyme which generates products of 30bp, 97bp and 140bp from a 267 bp amplicon. Samples harboring a V617F JAK2 mutation don't have the Bsa XI restriction enzyme leaving the 267 bp amplicon intact. Capillary electrophoresis is used to resolve the different sized amplicon products. Real time PCR using a mutation specific primer pair detects the absolute quantity by determining the copy number of the genomic DNA by using the $2^{-\Delta\Delta Ct}$ calculation, in this study. The PCR cycle in which a threshold signal is generated above the background noise is called the threshold cycle (Ct). Positive result means that the Ct value of the tested sample is ≤40.
Results: Sensitivity of real time PCR is as low as 0.01% (1 positive cell per 10,000 cells) whereas that of RFLP is 5.0% (5 clonal cells in 100 normal cells). Out of 254 samples, 31 samples were positive with real time-PCR of which only 24 were positive with RFLP; that is 77.4% concordance between 2 methods. In the remaining 7 cases, the results were either normal or indeterminate on RFLP whereas the real time-PCT $2^{-\Delta\Delta Ct}$ calculation in these subjects ranged from 0.02-0.4%. 4 cases with indeterminate results on RFLP were negative on real time-PCR.
Conclusions: This study suggests real time PCR as a more sensitive method for JAK2 mutation detection, which can also quantify the genomic DNA. The $2^{-\Delta\Delta Ct}$ method reduces the time needed for preparation of standards and making a standard curve. In addition it reduces the contamination risk, reagent usage and the overall cost by reducing the number of reactions run each time.

1908 RNA Preservation in FFPE Tissues Requires Pre-Analytical Standardized Processing.
G Bussolati. University of Turin, Italy.
Background: Preservation of RNA for Gene Expression profiling is notoriously poor in Formalin Fixed Paraffin Embedded (FFPE) tissues, thus hampering extended gene sequencing in routinely processed histo-pathological tissues.
Design: Our hypothesis was that RNA degradation in surgical biopsies is caused by RNAse activation before and during formalin fixation and that low temperature (4°C) could inhibit this activity and prevent degradation. In our Hospital (a large, pavillon hospital in Piedmont, Italy) the traditional habit of transferring specimens from the surgical theatre to the Pathology laboratory while immersed in large boxes filled with formalin was substituted by Under-Vacuum sealing (UVS) using the TissueSAFE™ apparatus. Specimens, routinely U.V. sealed immediately after surgical removal, were kept at 4°C for 1-72 h. until transfer. Grossing, fixation in Phosphate-buffered Formalin (PBF) and paraffin embedding followed. Selected specimens were processed by a 24 h. fixation in PBF at controlled temperature.
Results: UVS was well accepted by both Surgery and Pathology staff and this procedure, now in daily use since 2 years, assured proper histological and immuno-histochemical quality as well as RNA preservation (RIN values above 7). Fixation in PBF at controlled conditions improved RNA preservation and gene expression analysis of paraffin-embedded tissues.
Conclusions: Standardization of pre-analytical processing is mandatory for a proper preservation and processing of surgical biopsies. Their transfer in UVS assured standard quality for structural, antigenic and nucleic acids analysis.

1909 Choosing an Immunohistochemistry (IHC) System? A Comparison of 3 IHC Stainers and Polymers from Different Manufacturers.
Q Dai, ES Reisenbichler, MS Rasco, DK Horton, O Hameed. University of Alabama at Birmingham.
Background: IHC is routinely used in contemporary pathology practice and its quality depends upon many factors including IHC instruments and detection systems. The aim of this study was to compare the IHC results obtained using different open immunostainers and polymer detection kits.
Design: Different control sections for 9 antigens (CD3, CD20, CD45, CK, CK5/6, KI67, TTF1, BCL1, and S100) were sequentially evaluated by IHC utilizing 3 antibodies (Abs) from different sources [BIOCARE (BC), LABVISION (LV), DAKO (DK)], 3 different immunostainers (BC, LV, DK), and 3 different polymers (BC, LV, DK), generating 243 possible Ab/immunostainer/polymer combinations. The intensity (0-3+) and percentage of cells staining (0-100%) were used to generate an H-score (0-300). Technical issues (loss of tissue, failure of staining, no counterstain) were recorded as absent, minor (still interpretable), or major (not interpretable), while background staining was recorded as present or absent.
Results: There was variation in the staining of the different antigens when utilizing the unique Ab/immunostainer/polymer combinations from the same manufacturer (figure 1), with different overall mean H-scores for BC, LV, and DK (171, 199, and 218, respectively; P=0.019, paired ANOVA).
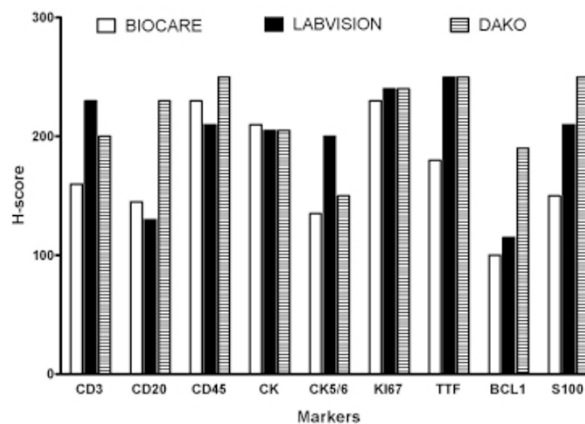
Comparison of staining between the 3 immunostainers (regardless of Ab/polymer) also showed different overall mean H-scores (175, 199, and 201, respectively; P=0.036, paired ANOVA), as did comparison between the 3 polymers (regardless of Ab/immunostainer) (194, 204 and 177, respectively; P=0.0003, paired ANOVA). The overall incidence of technical problems across immunostainers was 18%, 23%, and 20% for BC, LV, and DK, respectively (P>0.05, X^2) with major issues representing 43%, 26% and 19% of these issues, respectively (P>0.05, X^2). Background staining was seen in 15%, 14%, and 9% of cases utilizing the BC, LV, and DK polymers (P>0.05, X^2).

Conclusions: There are significant differences in staining results obtained using different IHC stainers and polymer detection kits. These findings, as well as others (e.g. cost of reagents, quality and timeliness of technical support), should be taken into consideration when selecting the optimal antibodies/immunostainers/detection systems for IHC.

1910 Patch TMA Construction Using Pre-Existing Slides as Source of Tissue When Paraffin Blocks Are Unavailable.
F-M Deng, Y Zhao, X Kong, P Lee, J Melamed. New York University Langone Medical Center, NY.
Background: Tissue microarray (TMA) has evolved as a useful platform for tissue based studies with the advantage of miniaturization permitting entire studies on single slides. This allows standardized experimental conditions on large numbers of cases for tissue based studies. Additionally, the "same slide" platform also facilitates image analysis techniques for more standardized interpretation. Construction of tissue microarrays however has required the original paraffin block to be available to provide donor tissue. Institutions that treat referral patients receive consultation slides from many different hospitals and laboratories and are therefore often limited on studies of these materials without the original paraffin block. We describe a technique for construction of intermediate density tissue microarray slides based on transfer of tissue from pre-existing routine slides provided for pathology diagnosis in situations where the original paraffin block is unavailable.
Design: A prostate cancer TMA was constructed using 20 cores from radical prostatectomy slides. Briefly, this technique entails removal of the coverslip on each slide and reinforcement of the tissue by covering with Mount-Quick liquid mounting medium. Once the medium has hardened, the attached tissue with its new scaffold may be "biopsied" using a tissue microarray needle (1.5 mm in diameter). The resultant biopsy disk is then transferred onto a recipient slide, with adhesion of the disc to the slide accomplished using heavy pressure. The utility of this patch TMA relies on preservation of morphology and antigenicity of the tissue for immunohistochemistry and confidence that it can be performed without substantial loss of tissue. We therefore tested this in comparison to a traditional TMA by applying a patch TMA on the same slide side by side next to a traditional TMA. The slide was then subject to immunohistochemical staining with antigen retrieval and assessed for expression of the antigen and loss of tissue.
Results: After immunohistochemistry, 19 of 20 cores were intact on the traditional TMA compared with 16 of 20 cores on the patch TMA. Expression of the marker (34BE12) was similar on both the patch TMA and traditional TMA.
Conclusions: Patch TMA represents a viable alternative for tissue-based immunohistochemical studies when paraffin blocks are unavailable. This may be a valuable tool for allowing use of archival slide material and enable a standardized TMA platform to be used when the slides sent for review from other institutions are the only source of tissue available.

1911 Immunocytochemical Staining for Cytokeratin 20 in Urine Cytology To Detect Neoplasia: Comparison with FISH Analysis.
KA Devitt, G Leiman, J Mitchell. Univ of Vermont College of Medicine, Burlington.
Background: Urine cytopathology, widely used in screening for urothelial neoplasia, has high specificity (95%) but low sensitivity (40-80%). At this institution, cases are sent for fluorescent in situ hybridization (FISH) analysis by physician request, predominantly on cases classified as atypical or suspicious on cytologic evaluation; FISH is expensive and time-consuming. Recent literature suggests that cytokeratin 20 (CK20) immunohistochemical staining can identify urothelial neoplasia. CK20 staining is less expensive and more widely available than FISH. CK20 immunocytochemical staining and FISH results in 100 consecutive exfoliative cytopathology cases are correlated in this study.
Design: One hundred consecutive, archived Papanicolaou-stained urine cytology cases previously sent for FISH analysis were retrieved. Atypical cell groups were photographed prior to restaining with CK20 (Ks20.8, LabVision). Blinded to FISH results, slides were examined for immunostaining pattern and categorized as positive, negative, or indeterminate. CK20 and FISH results were correlated using simple statistics.
Results: Cytologic results on cases sent for FISH comprised 70 atypical, 18 negative, 7 suspicious and 5 malignant cases. FISH testing was negative in 71, positive in 20 and suspicious in 8 cases. One case had insufficient material for FISH. CK20 staining was negative in 72 cases, positive in 26. Two cases with indeterminate results were not included in analysis. The results of FISH analysis were used primarily as the gold standard for comparison. In discordant cases and those with suspicious FISH results, clinical follow-up, subsequent cytopathology or surgical specimens were reviewed. In two such cases, no further results were available; those cases were removed from analysis. Of the remaining 96 cases, there were 3 false negative and 4 false positive results. The sensitivity of CK20 staining was 87.5% and the specificity was 94.4%.
Conclusions: Based on 87.5% sensitivity and 94.4% specificity in this study, the use of CK20 as a marker of urothelial neoplasia has potential for practical use in the laboratory. CK20 is more widely available, cost effective, and has a faster turnaround time than FISH analysis. Potential drawbacks include varying levels of individual experience with stain interpretation, distraction by and misinterpretation of CK20 positive superficial urothelial cells, and inability to recognize atypical cell groups on stained slides.

1912 FGFR3, PIK3CA and BRAF Mutations in Urine Cytology Specimens.
A Hasanovic, GV Iyer, DB Solit, H Al-Ahmadie, A Heguy, O Lin. Memorial Sloan-Kettering Cancer Center, New York, NY.
Background: Urothelial carcinoma is a common malignancy with variable biology and natural history. Prior studies have shown that the most common somatic mutations found in UC include FGFR3 and PIK3CA. The development of targeted therapies exploiting somatic mutations, translocations, and amplifications has served as a platform for new treatment protocols. This study is designed to evaluate if cytology specimens represent a suitable material to select patients for target therapy, given that urine cytology is a highly specific and relatively sensitive in the diagnosis of high grade UC and it is relatively easy to obtain. Clinico-pathological findings were also analyzed.
Design: Thirty cases of histologically proven UC and matching urine cytology material were identified at our institution. The cytology specimens were frozen, methanol fixed, cytospin unstained slides. The contents of one cytospin slide and a thick section of matching FFPE tissue were submitted to whole genome amplification. Samples were analyzed using the Sequenom platform for FGFR3, PIK3CA and BRAF mutations using probes previously validated with frozen specimens of UC. All traces for mutation findings were manually reviewed. Clinico-pathologic correlation was performed.
Results: The frequency of mutations in cytology specimens is listed in the table 1. Correlation with the tumor sections showed matching FGFR3 mutation in cytology and surgical specimen in one case, whereas 4 pairs of specimens had discordant FGFR3 mutations. Additionally, 9 cytology specimens showed the presence of a mutation (S371C) not seen in the tumor sections. Concordant PIK3CA mutation was present in both cytology and histology specimens only in one case, while 4 cases showed discrepant mutational status. BRAF was not detected in any cytology or surgical specimen. Correlation of the molecular status with the clinical findings showed that FGFR3 mutation was detected mostly in non-invasive UC with a papillary component, while PIK3CA mutation was found in superficial as well as muscle invasive UC with a papillary component.

Frequency of mutations in cytology specimens

Mutation	N	Proportion
FGFR3	12	40%
PIK3CA	3	10%
BRAF	0	0%

Conclusions: Mutations can be detected in urine specimens using the Sequenom platform, however the specificity is still low and the FGFR3 S371C mutation represents a frequent false positive result in cytology specimens using this assay. FGFR3 and PIK3CA mutations are associated with a papillary architecture in the tissue sections and FGFR3 mutation was only seen in non-invasive carcinomas.

1913 SIVQ Image Analysis: A High-Throughput Morphology Discovery Tool for Surgical Pathologists.
J Hipp, J Cheng, J Hanson, W Yan, J Rodriguez-Canales, J Hipp, M Tangrea, MR Emmert-Buck, S Han, S Hewitt, J Monaco, A Madabhushi, U Balis. University of Michigan, Ann Arbor; National Institutes of Health, National Cancer Institute, Bethesda, MD; Rutgers University, Piscataway, NJ.
Background: Spatially-Invariant Vector Quantization (SIVQ) is an image analysis algorithm based on morphologic and histopathologic pattern matching. Training to identify features is not required and is as simple as clicking on a particular morphologic feature. It has very high selectivity as compared to conventional morphometric approaches; and can be performed in a matter of minutes on a laptop.
Design: SIVQ was used to identify breast calcifications, microorganisms, breast epithelium and stroma, normal esophagus and tumor.
SIVQ was also integrated with an existing high-performance algorithm (probabilistic pairwise Markov model, PPMM) for the identification of prostate cancer.
SIVQ was integrated into the workflow of the Arcturus XT laser capture microdissection (LCM) instrument to dissect frozen esophageal normal and tumor tissue.
Results: SIVQ was used to analyze breast biopsy cases of patients with ultrasound densities, and count the percentages of stroma and epithelial components. The total run-time to identify and "paint" the epithelium and stroma of 500 breast images with SIVQ was under 15 hours.
SIVQ was integrated it into an existing algorithm (PPMM) for the identification of prostate cancer. By combining SIVQ's ability to identify the malignant morphology with PPMM's ability to identify abnormal luminal architecture, we show that the synergistic algorithm's cancer detection capability is superior to that of either algorithm individually. This approach is unique in that it models the "thought process" of a pathologist working up a prostate cancer case.
SIVQ was then applied to LCM. Samples of normal and tumor epithelium were profiled on the Affymetrix Genechip and compared to the gold standard, LCM by hand. Dendrograms, were highly similar to each other, thus supporting equivalency between the two dissection methods (manual vs. automated).
Conclusions: Here we demonstrate that SIVQ serves as a high-throughput morphologic analysis and selection tool to assist surgical pathologists.
SIVQ enables high-throughput clinical studies, such as extraction of percentages of specific cell types from whole-slide images.
Integration of SIVQ with LCM significantly improves the work-flow of microdissection by: 1) enabling the collection of large preparative amounts of morphologically-constrained biologic material for high-throughput expression studies and 2) significantly decreasing human-contact machine time.


1914 Ischemic Time Impacts Biological Integrity of Phosphoproteins in PI3K/Akt, Erk/MAPK, and p38 MAPK Signaling Networks.
TR Holzer, AD Fulford, AM Arkins, JM Grondin, CW Mundy, A Nasir, AE Schade. Eli Lilly and Co., Indianapolis, IN.
**Background:** It is well-established that protein post-translational modifications, such as phosphorylation, are labile events dynamically regulated by opposing kinase and phosphatase activities. Therefore, preanalytical variables such as ischemic time before fixation can have a significant impact on the ability to interrogate signaling pathways in tissue.

Design: We performed immunohistochemical analysis of p-PRAS40 (Thr246), p-p70S6 kinase (Thr389), p-ribosomal protein S6 (Ser240/Ser244), p-Erk (Thr202/Tyr204), p-BAD (Ser112), p-p38 MAP kinase (Thr180/Tyr182), and p-MAPKAP kinase 2 (Thr334) in human cell line xenografts from lung (A549), brain (U87MG), ovary (A2780), and prostate (PC3) tumors. In order to replicate real-world practices, the tissues were subjected to ischemic times ranging from 0 (baseline) to 24 hours before fixation in formalin. Staining was quantified by a positive pixel counting algorithm, and stability profiles were generated for each phosphoprotein in each tissue.

Results: Phosphoprotein stability profiles show either an increase (n=1), an initial increase followed by a decrease (n=7), a decrease (n=10), or a relatively stable level of staining (n=6). Figure 1 shows representative stability profiles for p-MAPKAP kinase 2 in all four tissues.
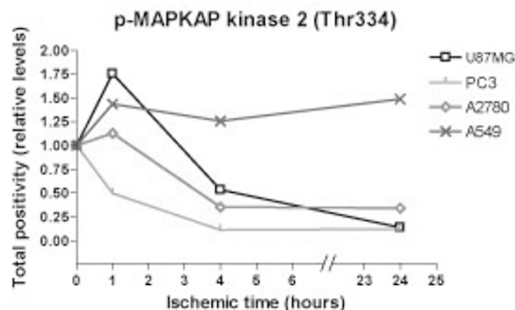
In Figure 2, representative stability profiles for all phosphoproteins in U87MG are shown.
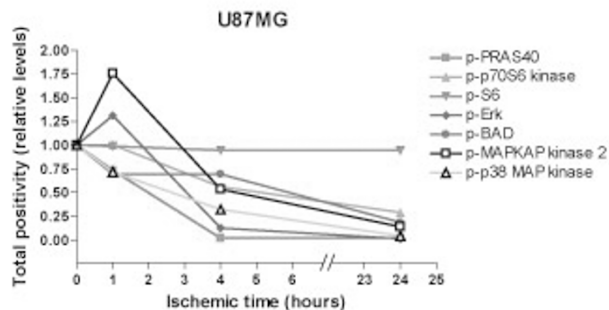
Conclusions: Two key concepts emerge from this analysis: (a) the stability of a given phosphoepitope varies significantly across multiple tumor types, and (b) the stability of different phosphoepitopes within a given tumor type is variable. These results highlight the importance of proper tissue acquisition and rapid fixation to preserve the biological integrity of signal transduction pathways that will guide therapeutic decision making.

1915　Use of a Novel FISH Assay as a Diagnostic Adjunct for Extraskeletal Myxoid Chondrosarcoma.
D Huang, JA Bridge. University of Nebraska Medical Center, Omaha.
Background: Approximately 75% of extraskeletal myxoid chondrosarcomas (EMC) are characterized by a recurrent t(9;22)(q22;q12) translocation resulting in the fusion of the *EWSR1* gene on chromosome 22 with the *NR4A3* gene on chromosome 9. Less frequently, the *NR4A3* gene is fused with a different gene partner; cytogenetic variant translocations t(9;17)(q22;q11), t(9;15)(q22;q21) and t(3;9)(q11-12;q22) with associated *NR4A3-TAF15, NR4A3-TCF12* and *NR4A3-TFG* fusions respectively have been described. EMC may be difficult to distinguish from other cartilaginous or myxoid lesions. As a diagnostic aid, we constructed a FISH probe set that can: 1) be performed on formalin-fixed, paraffin-embedded (FFPE) tissue; and, 2) identify potential unusual variant translocations or cryptic rearrangements involving the *NR4A3* locus in EMC.
Design: Probe cocktails of selected BAC clones were developed to assess the *NR4A3* locus as a break-apart rearrangement. After establishing the specificity of the probes [on normal peripheral blood lymphocytes and 9;22 rearranged EMC metaphase cells], we evaluated cytologic touch preparations or FFPE tissue sections of four cytogenetic and/ or molecular cytogenetic characterized EMC specimens using two-color FISH assays. *EWSR1* FISH was performed on one EMC case exhibiting a 9;15 translocation.
Results: *NR4A3* abnormalities were detected by FISH in all four EMCs. Detection of equivalent split red and green signals in three cases indicated a balanced translocation event involving *NR4A3*. Loss of one of the proximal *NR4A3* probe signals in the remaining EMC case suggested the presence of an unbalanced structural rearrangement. Subsequent *EWSR1* FISH on this same case similarly showed loss of only the distal probe signal consistent with the conclusion of the presence of an unbalanced rearrangement [der(22) of the 9;22 translocation] in this case. The FISH findings with this novel *NR4A3* FISH probe set were concordant in all four EMCs that also had informative results for *EWSR1* FISH or conventional karyotyping.
Conclusions: FISH analysis with this newly designed probe set is a reliable and specific method for detecting all variant translocations involving the *NR4A3* gene locus in

routinely processed tissue (including FFPE tissue) and it may serve as a useful diagnostic aid in distinguishing EMC from clinicohistopathologically similar lesions.

1916　HPV Detection in Head and Neck Cancer Using an Automated In Situ Hybridization Approach To Decrease Turnaround Time.
PB Illei, WH Westra. Johns Hopkins Medical Institutions, Baltimore, MD.
Background: The human papillomavirus (HPV) is driving the escalating incidence of oropharyngeal cancer, and its detection in head and neck squamous cell carcinoma is recognized as a highly relevant clinical biomarker. HPV in-situ hybridization is readily applied to routinely processed tissues facilitating its use in most diagnostic laboratories, but reproducibility is limited by technical inconsistencies. Automation could enhance standardization across diagnostic laboratories, and decrease turnaround time.
Design: An automated in situ hybridization method using the INFORM HPV III Family 16 Probe (Ventana Medical Systems, Tucson, AZ) was used to evaluate 311 head and neck squamous cell carcinomas (HNSCCs). These cases had been previously evaluated using a manual method with an HPV16 genome specific probe (Dako, Carpintera, CA) as part of clinical care (64 cases) or research (267 cases constructed onto a tissue microarray). Results for the two detection systems were compared.
Results: The automated method detected HPV in 52 of 64 (81%) clinical samples and 43 of 267 (16%) tissue array samples. There was 98% concordance between the two detection systems with only 7 discordant cases: 5 cases that were HPV-negative by the manual assay were HPV-positive with the automated assay, and 2 cases that were positive by the manual assay were negative with the automated assay.
Conclusions: HPV detection utilizing an automated in situ hybridization system can detect HPV with a very high degree of fidelity. The assay run time can be reduced to 7-8 hours from 16-24 hours. By diminishing the impact of technical inconsistencies, high throughput automation promises to decrease turnaround time for large case volumes, enhance standardization across diagnostic laboratories, and improve reproducibility among clinical trials.

1917　Select microRNA Profiles of Patients with Chronic Lymphocytic Leukemia.
P Kaur, CL Bartels, HA Bentley, GJ Tsongalis. Dartmouth-Hitchcock Medical Center, Lebanon, NH.
Background: MicroRNAs (miRNAs) are small endogenous, non-coding 22-nucleotide regulatory RNAs found in plants and animals. miRNAs modulate hematopoietic lineage differentiation and play important gene-regulatory roles during development by pairing with target mRNAs to specify posttranscriptional repression of these messages. In human chronic lymphocytic leukemia (CLL), the most common leukemia in the western world, mice- model studies have shown dysregulated expression of miR-15a, miR-16, and mir 29-a to cause a disease simulating human CLL. MiRNA 181, is a putative regulator of B-cell differentiation in mice and its dysregulated expression has been associated with disease progression in a select population of human CLL. In this study we evaluated these miRNA profiles from B-cell enriched prospective CLL samples.
Design: In the present study, nineteen RNA samples, representing 18 CLL patients, were extracted from fresh peripheral blood specimens. The patient's ages ranged from 46 to 90 years and ten of these were treated previously while 8 were untreated. Samples were collected at different time points between August 2009 and September of 2010. The samples were enriched for B-cells using the RosetteSep Human B Cell Enrichment Cocktail (StemCell Technologies, Vancouver, BC, Canada) and total RNA was extracted using the *mir*Vana™ miRNA Isolation Kit (Ambion). Expression of miR15a, miR16-1, miR29a, miR181a, and U47 (an endogenous control) in each sample was determined using TaqMan® MicroRNA Assays (Applied Biosytems). In addition, expression of these miRNAs was determined in B cells from normal samples. The DC_T of the normal ($C_{Tnormal} - C_{Tendogenous\ control}$) and CLL samples ($C_{TCLL\ sample} - C_{Tendogneous\ control}$) were calculated, and relative comparison of normal and CLL samples was made using the DDC_t method ($DC_{TCLL\ sample} - DC_{Tnormal}$).
Results: In this study, we found that there is an upregulation of miR29a and, down-regulation of miR15a and miR16-1 expression. Interestingly, miR 181a was downregulated in all CLL patients compared to normal.
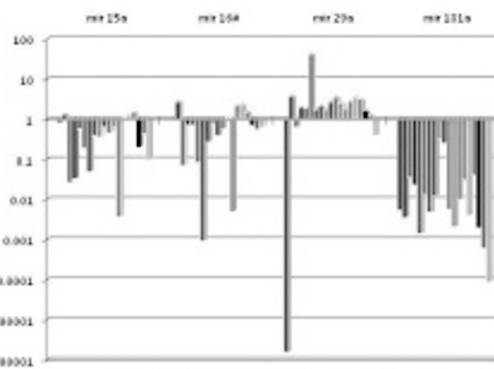

Figure 1. Expression of select miRNAs from B cells of fresh peripheral blood samples.

Conclusions: Our preliminary results show that miRNA 181a expression levels in CLL patients differs from that of normal patients and is a likely candidate for further evaluation for its role in disease progression in CLL.

1918 Massarray Technology: High Throughput Method for Unlocking the Presence of Recurrent Fusion Gene in Cancer.

MB Lambros, R Natrajan, R Vatcheva, H Gohlke, M Plant, S Muller, JS Reis-Filho. ICR, London, United Kingdom; Sequenom GmbH, Hamburg, Germany.

Background: Fusion genes result from chromosomal structural rearrangements and play pivotal roles in the biology of many solid tumours. We and others have recently demonstrated that breast cancers harbour fusion genes, however most of the fusion genes identified in breast cancer appear not to be recurrent with the exception of ETV6-NTRK3 in secretory carcinomas and MYB-NFIB in adenoid cystic carcinomas. Conventional approaches to determine whether a fusion gene is recurrent (e.g. fluorescence in situ hybridisation (FISH) and reverse transcriptase PCR (RT-PCR)) are either labour intensive or prone to false positive results. The aim of our study was to develop a high throughput method to investigate multiple samples for the presence of novel fusion genes based on the MassArray technology (iPLEX® assay).

Design: Nine breast cancer cell lines previously subjected to massively parallel sequencing and known to harbour 10 specific fusion genes previously validated by Sanger sequening and FISH were used as the study group. RNA was extracted from 126 formalin fixed paraffin embedded (FFPE) breast cancers, 9 breast cancer cell lines and HeLa cells, and converted to cDNA. Small amplicons (70-150bp) were designed based on the breakpoint positions within the cDNA sequence of a given fusion gene, followed by a single primer extension from one partner of the fusion gene to the other. Two pairs of extension primers were used to extend from one partner of a given fusion gene to the other and vice versa. A multiplex of 13 PCR amplicons, were used to identify 13 fusion genes discovered recently in breast cancer cell lines. Positive results were validated by RT-PCR.

Results: MassArray displayed a sensitivity of 98.9%, a specificity of 95.2%, a positive predictive value of 38.6% and a negative predictive value of 99.9% to detect all fusion genes tested. All positive results were validated by RT-PCR and sequencing. Fusion genes were accurately detected in cDNA dilutions of up to 1:5.000. Although no recurrent fusion genes were detected and validated in the small cohort of primary tumours analysed in this study, all fusion genes were accurately detected in the panel of cell lines used.

Conclusions: The high level of sensitivity of the MassArray assay suggests that such high throughput assay can be used as a screening tool to investigate the presence of known fusion genes. Further work is required to minimise the number of false positive results. The small PCR amplicons (70-150 bp) used for the MassArray assay facilitates the usage of FFPE tissue samples.

1919 A Novel Break Apart Fluorescence In Situ Hybridization Probe Using an Extra Signal Strategy Shows Superior Sensitivity and Specificity in Detecting MYC Translocations.

ME Law, ED McPhail. Mayo Clinic, Rochester, MN; Mayo Clinic, Rochester.

Background: The identification of MYC translocations is important for the classification and management of lymphomas. Interphase fluorescence in situ hybridization (FISH) using breakapart (BAP) probes is widely used to determine the presence or absence of this translocation. Presently available commercial MYC BAP probes are prone to either false negative results due to lack of coverage for minor breakpoints (BVR2 breakpoint cluster region; Dako [DK]), or false positive results due to the presence of a large gap (1.6MB; Abbott Molecular [AM]). To overcome these limitations, we developed a MYC BAP probe ((homebrew [HB]) with a small gap (181kB) and a large distal region that spans the minor breakpoint region.

Design: In order to evaluate the sensitivity and specificity of these 3 MYC BAP probes (DK, AM and HB), interphase FISH was performed using each probe on formalin fixed paraffin embedded (FFPE) sections of 1 normal tonsil (negative control), Raji cell line (positive control), and 6 B-cell lymphomas whose MYC translocation status had been previously determined using the AM probe in our clinical practice. We used 3 lymphoma cases lacking a MYC translocation, 1 possessing a typical MYC translocation involving the major breakpoint region, and 2 possessing MYC translocations involving different minor breakpoint regions. Signals that were not overlapped or touching were categorized as translocated.

Results: Using this scoring method normal tonsil showed no split signals using the DK and HB probes, while 25/500 (5%) showed a split signal (false positive) using the AM probe. The lymphomas without a translocation and the lymphoma with a typical translocation were correctly analyzed using all 3 probe sets. Both lymphomas with MYC translocations involving the minor breakpoint region were positive using the AM and HB probe sets, while 1 case (which possessed the more distal breakpoint) was negative using the DK probe.

Conclusions: The homebrew MYC BAP FISH probe showed superior specificity to the AM probe and superior sensitivity to the DK probe. It is easy to score and is amenable to routine clinical use. The strategy of designing a BAP probe with a small gap to minimize false positive results and a large flanking probe to minimize false negative results may be applicable for detecting other translocations with varying breakpoints.

1920 DOE Methodological Evaluation of Efficacy of Residual Paraffin Removal during IHC Process Development.

S Liu, G Nuttman, J Erickson, G Toland, T Phillips, S Webster, R Welcher. Dako North America, Carpinteria, CA.

Background: Non-toxic and biodegradable Histoclear™ is widely used as a xylene substitute for immunohistochemical (IHC) deparaffinization and post-IHC clearing during permanent coverslipping. However, Histoclear has been reported to be a less efficient clearing agent and can fail to completely remove paraffin from the specimens. We have observed that residual paraffin can be trapped in cell structures, especially in the nuclei of some formalin-fixed, paraffin-embedded (FFPE) cell pellets when the sections are subjected to heat pretreatment. This results in an artifact which is manifested as an apparent patchy distribution of IHC staining and a loss of clearly distinguishable cell margins. Since both heat pretreatment and the uses of Histoclear are common practices in IHC, we investigate which combination of these factors will reduce the incidence of paraffin artifacts.

Design: This study employs design of experiments (DOE) methodology to compare the aforementioned procedures for the treatment of FFPE cell pellet sections before and after IHC staining. Three factors, deparaffinization, heat, and post-IHC clearing were chosen for the 2^k factorial experimental design. The contribution of any one factor and the interactive contribution of any two factors of the procedure were evaluated monitoring the level of residual paraffin. Data was analyzed by Minitab® software.

Results: The results confirmed that 1) Heat pretreatment cause a major increase in residual paraffin staining artifact, 2) Use of Histoclear in deparaffinization procedures was not as effective for removal of paraffin as xylene when heat pretreatment was subsequently performed and 3) Post-IHC clearing with Histoclear prior to permanent mounting of coverslips was essential to achieve a satisfactory solution of quality staining with minimal residual paraffin.

Factors and Levels

Factor	Description	Low level of factors (-)	High level of factors (+)
A	Deparaffinization	Histoclear	Xylene
B	Heat	No	Yes
C	Post-IHC clearing with Histoclear	No	Yes

Two-level 3 factor full factorial DOE results

Run	Combination	Factor A	Factor B	Factor C	Score
1	-1	-	-	-	1.5
2	a	+	-	-	1
3	b	-	+	-	70.5
4	ab	+	+	-	12.5
5	c	-	-	+	0
6	ac	+	-	+	0.5
7	bc	-	+	+	0
8 = 2x2x2	abc	+	+	+	0

Conclusions: DOE technique is a powerful tool for the systematic evaluation of several concurrent response variables and the efficient improvement of process development. This study recommends a higher-quality and eco-friendly procedure using the combination of Histoclear deparaffinization and post-IHC clearing when residual paraffin is observed within cell structures.

1921 Quantifying Small Lymph Node Metastases in Breast Cancer.

C Luedtke, S Patil, L Tan, E Brogi, D Giri. Memorial Sloan-Kettering Cancer Center, New York, NJ; Memorial Sloan-Kettering Cancer Center, New York, NY.

Background: The 2010 AJCC staging of breast cancer axillary nodal metastases classifies isolated tumor cells (ITCs) as clusters of cells not greater than 0.2 mm or nonconfluent clusters not exceeding 200 cells in a single histologic lymph node cross section. Because this distinction can impact patient management and prognosis, we evaluated the diagnostic reproducibility of counting cells and measuring tumor clusters using hematoxylin and eosin (HE) and cytokeratin (CK) stains on glass and digitally scanned slides.

Design: Lymph nodes were selected from a cohort of 83 patients initially node negative that converted to node positive following deeper levels with HE and CK stains. 104 lymph node cross sections taken from these 83 patients were assessed twice by reviewer 1 and once by reviewer 2. Each reviewer evaluated a glass and corresponding digital slide, both stained with HE and CK. Spearman correlations were used to compare these different methods of pathological evaluation in counting cells and measuring tumor cluster size. For each method, the intra and inter observer variability was also calculated.

Results: The comparison of cell counts and cluster size measurements for the various combinations of glass and digital slides with HE and CK stains are listed in Table 1. The intra and inter observer variability are summarized in Table 2.

Table 1

Methods Compared	Cell Counts*	Largest Cluster Size*
Glass HE - Digital HE	0.87	0.85
Glass CK - Digital CK	0.91	0.93
Glass HE - Glass CK	0.59	0.76
Digital HE - Digital CK	0.52	0.75

*Values represent Spearman correlation

Table 2

Assessment Method	Intra Observer Variability*		Inter Observer Variability*	
	Cell Counts	Size^	Cell Counts	Size^
Glass HE	0.85	0.93	0.81	0.85
Digital HE	0.92	0.96	0.77	0.89
Glass CK	0.99	0.93	0.98	0.92
Digital CK	0.99	0.99	0.98	0.98

*Values represent Spearman correlation; ^Measurement is of the largest tumor cluster

Conclusions: In this study, the highest correlation for counts and measurements is observed between glass and digital slides each stained with CK. The lowest correlation for counts and measurements is between HE digital slides and CK digital slides. For counts, the evaluation methods with the least intra and inter observer variability are CK stained slides, regardless of whether a glass or digital slide is used. For measurements on the other hand, the intra and inter observer variability is least for digital slides with CK.

1922 Decalcification with Nitrical® Can Preserve DNA/RNA for *In Situ* Hybridization and Proteins for Immunohistochemmistry in Formalin-Fixed Paraffin Embedded Tissues.

KA Mead, J Tull, NM Drotar, S Zhang. SUNY Upstate Medical University, Syracuse, NY.

Background: Decalcification is a common procedure performed on histologic specimens. However, the conventional decalcifier, RDO, does not preserve DNA or RNA well and therefore render failures in various molecular assays, including chromogenic in situ hybridization (CISH) and fluorescent in situ hybridization (FISH). As DNA/RNA based molecular assays are becoming increasingly employed in the practice of pathology, it is important to discover a decalcifier that can preserve DNA/RNA but does not affect proteins for immunohistochemistry (IHC). In this study, we tested Nitrical®, a rapid decalcifier, in its preservation of RNA and DNA for molecular assays as well as proteins for IHC.

Design: Selected tissues of bone marrow, colon or skin were treated in parallel with Nitrical® or RDO for 30 min after formalin fixation and before paraffin-embedding. Commonly-used CISH probes for kappa chain, lambda chain and HPV, and FISH probes for *HER2* and *EGFR* were tested on the treated tissues. In addition, 15 antibodies (pancytokeratin, AE1/AE3, CAM5.2, TTF-1, CDX-2, S100, EMA, P16, SMA, kappa, lambda, LCA CD20, CD34 and CD68) for a variety of proteins were also tested on same tissues. Intensities of *in situ* signals or IHC stains as well as backgrounds of both decalcifiers were compared.

Results: There were not any CISH or FISH signals identified in the RDO treated tissues. However, both CISH and FISH showed moderate to strong signals in Nitrical® treated tissues with a clean background. Although all the IHC in RDO treated tissues demonstrated staining (1-3+), the intensities in Nitrical® treated tissue are overall stronger (2-3+). It was also noted that background stains of IHC in Nitrical® treated tissue was slightly higher than that of RDO in occasional cases.

Conclusions: Nitrical®, a rapid decalcifier, can preserve RNA, DNA and proteins for CISH, FISH and IHC assays, respectively, in formalin-fixed paraffin embedded tissues. In the age of rapid development of molecular studies, Nitrical® should be considered to replace the conventional decalcifier, RDO, in routine pathology practice.

1923 Determining the Protein Profile of Prostate Cancer Samples Harboring the ERG Rearrangement Using MALDI Imaging Mass Spectrometry.

R Menon, K Schwamborn, P Nikolov, M Braun, RM Caprioli, S Perner. Institute of Pathology, University Hospital Bonn, Germany; Mass Spectrometry Research Center, Vanderbilt University Medical Center, Nashville.

Background: The ERG gene rearrangement is seen in a majority of patients suffering from prostate cancer (PCa). This gene fusion has been characterized at the genomic level, but much is yet to be done at the protein level. The aim of our study was to molecularly determine a protein profile specific to PCa samples harboring the ERG rearrangement, using MALDI imaging mass spectrometry.

Design: We characterized 94 fresh frozen PCa samples, from a consecutive prostatectomy series, for ERG rearrangement status by fluorescence in-situ hybridization (FISH). 68 samples were positive and 26 samples were negative for the ERG rearrangement status. The samples were further processed for MALDI imaging as follows: Fresh frozen prostate sections (12 μm) were thawed and mounted onto conductive glass slides and fixed in graded ethanol washes. Matrix application was achieved by spotting sinapinic acid onto the tissue in an array pattern using an acoustic reagent multispotter (Portrait 630, Labcyte). Samples were analyzed utilizing an Autoflex speed MALDI-TOF mass spectrometer (Bruker). Data analysis was performed by using the ClinProTools 2.2 and FlexImaging 2.1 software (Bruker).

Results: The analyzed PCa tissue revealed on average 156 peptides and proteins in the mass range from *m/z* 2,000-20,000. Distinctive differences in peak patterns could be identified between ERG rearranged and non-rearranged samples. Combining five peaks in a genetic algorithm based model resulted in an overall sensitivity of 91.2% and a specificity of 73.1% using the ClinProTools 2.2 and FlexImaging 2.1 software. For example, two proteins (*m/z* 9076 and 9750) had significantly higher expression in samples with ERG rearrangement.

Figure 1 : Two proteins (marked with *, m/z 9076 and 9750) showing significantly higher expression in samples with ERG rearrangement

RED- ERG rearranged (n=68)
GREEN- ERG non-rearranged (n=26)
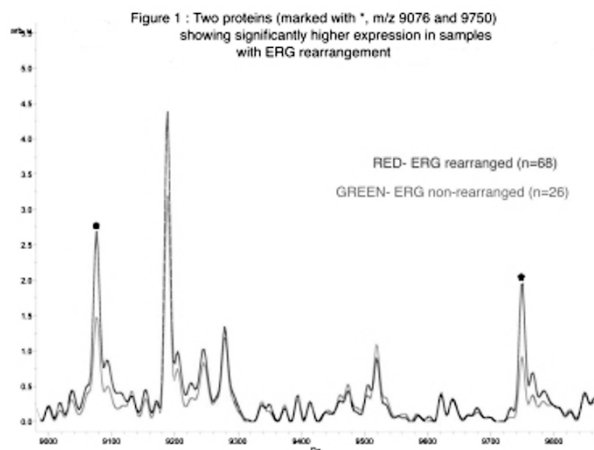
Conclusions: This is the first study investigating the protein profile specific for the ERG rearrangement in PCa. Identifying the differentially expressed proteins and validation using western blot and IHC, will provide further insight into the downstream protein signaling of the ERG rearrangement dependent PCa.

1924 In Situ Hybridization Detection of Dematiaceous Fungi in Formalin-Fixed, Paraffin-Embedded Sinonasal Specimens Using a Wide-Spectrum Oligonucleotide Probe.

KT Montone, VA LiVolsi, MD Feldman, I Nachamkin. University of Pennsylvania, Philadelphia.

Background: Dematiaceous fungi are a diverse group of "darkly" pigmented fungi which contain melanin in their cell walls and are commonly found in soil worldwide. While morphology and histochemical stains may aid identification in tissue sections, these means for species identification are not specific. In situ hybridization (ISH) for abundant fungal rRNA sequences may provide a means for detecting dematiaceous fungi and differentiating them from other clinically important filamentous fungi such as *Aspergillus sp., Paecilomyces sp,* and *Fusarium sp*. In this study, we report a rapid ISH assay for detecting dematiaceous fungi in formalin-fixed, paraffin-embedded tissue specimens.

Design: 29 patients with culture proven sinonasal dematiaceous fungal infections were utilized. These included *Alternaria sp.* (10), *Bipolaris sp.* (5), *Curvularia sp.* (10), *Cladosporium sp.* (1); *Scopulariopsis sp.* (1); *Scedosporium prolificans* and dematiaceous species, not otherwise specified (1). Rapid (<2.5 hour) ISH was performed using a 24 base oligonucleotide biotin-labeled DNA probe targeting the fungal rRNA gene sequences of a variety of dematiaceous fungi. By GenBank BLAST analysis, this sequence was shown to have 100% homology to nucleic acid sequences of a variety of fungi in the Phylum Ascomycota including *Curvularia sp.* and *Bipolaris sp.* and as well as uncultured soil fungi.

Results: ISH revealed positivity in 24 of 29 culture proven cases of dematiaceous fungal infection. The five negative cases included 2 *Bipolaris sp*, 2 *Curvularia sp*. and 1 case of *S. prolificans*. Two of the negative specimens had undergone decalcification in HCl-based decalcification solution prior to tissue processing. The dematiaceous fungal specific probe did not hybridize to culture positive examples of *Rhizopus sp., Aspergillus sp, Fusarium sp., Paecilomyces sp., H. capsulatum, Candida sp.,* and *B. dermatitidis*.

Conclusions: ISH can rapidly detect several human disease-related dematiaeous fungi and differentiate them from other medically important filamentous fungi such as Zygomyces, Aspergillus, Fusarium and Paecilomyces which are often clinically treated differently. This method can be performed rapidly and is useful for fungal identification in routinely processed tissue specimens. ISH using probes targeting a variety of fungal pathogens will be useful for triaging tissue based filamentous fungal infections in which fungal cultures are not available.

1925 Significantly Increased Detection Rate of High Risk Cytogenomic Markers by Interphase FISH on Enriched Plasma Cells.

R Muddasani, M Zhao, LV Abruzzo, JM You, LJ Medeiros, D Lovshe, G Lu. UT MD Anderson Cancer Center, Houston, TX.

Background: Accurate detection of high risk cytogenomic markers is clinically important for the design of appropriately therapy in patients with plasma cell myeloma (PCM). However, plasma cells in routine bone marrow (BM) aspirate samples are often diluted by blood negatively impacting our ability to detect cytogenomic markers by fluorescence in situ hybridization (FISH). The aim of this study was to improve the sensitivity of detection of cytogenomic markers in PCM patients by FISH using enriched plasma cells derived from BM aspirate samples.

Design: Plasma cells from BM aspirates, collected from 20 patients, were enriched using a magnetic cell sorting procedure (Miltenyi Biotec Inc. California) manually allowing for selection of CD138+ cells. iFISH was performed on enriched plasma cells using a standard laboratory protocol. FISH probes in this study were selected to detect high risk cytogenomic markers in PCM: del(17p13)/*TP53*, del(13q14)/*Rb1*, amp(1q21)/*CKS1B*, and *IGH* rearrangement. Cases positive for *IGH* rearrangement were followed up using probes for *IGH/FGFR3* and/or *IGH/MAF*. A total of 200 interphase nuclei were analyzed for each sample. FISH studies was also performed on paired samples from the same cases prior to plasma cell enrichment.

Results: Plasma cell counts in the enriched samples ranged from 31% to 93%, compared with 1% to 18% in the pre-enriched samples. Therefore, the enrichment procedure substantially increased the purity of the plasma cell population. High-risk cytogenomic markers were detected in 12/20 (60%) enriched samples compared with 3/20 (15%) pre-enriched samples, yielding a 4 times higher detection rate in the enriched specimens. Of the 12 iFISH-positive cases detected, 5 were positive for *TP53* deletion (25%), 4 for *Rb1* deletion (20%), 4 for *CKS1B* amplification (20%), and 5 for *IGH* rearrangement (25%). Of the 5 cases positive for *IGH* rearrangement, 2 were positive for *IGH/CCND1*, 1 for *IGH/MAF*, 1 with del(*IGHV*), and 1 with no specific *IGH* rearrangement. Of the 3 FISH-positive cases from pre-enriched samples, 2 (10%) were positive for deletion *TP53*, 2 (10%) for deletion *Rb1*, 1 (5%) for *CKS1B* amplification, and 1 (5%) for *IGH* rearrangement (5%).

Conclusions: FISH on CD138-enriched plasma cells significantly increases the detection rate for high-risk cytogenomic markers in PCM. Our data suggest that application of this plasma cell enrichment method in the clinical cytogenetic laboratory is useful for the workup of PCM bone marrow aspirate samples.

1926 A Novel Method To Procure Fresh Prostate Tissue for Viable Epithelial Cells.
B Palla, H Zhang, J Huang. University of California at Los Angeles; Anhui Medical University, Hefei, China.
Background: Cancer research depends on tumor models such as cell culture and mouse models but results from those studies need to be confirmed in human tissue. Archival human tissue is stored either as frozen tissue or in paraffin blocks, neither of which are suitable for studies that require live cells. We have designed a strategy to obtain fresh prostate tissue to prepare live prostate epithelial cells.
Design: 1. Prostatectomy specimens were sectioned into 3-4 mm thick slices from base to apex.
2. Levels 2 and 4 were divided into 4 quadrants and each quadrant was divided into superior and inferior halves. The superior half was submitted for frozen section to identify cancer versus benign tissue, while the inferior half was kept fresh on ice. The fresh tissue was then matched up with the frozen tissue section on the slide, and the fresh benign tissue was separated from cancer.
3. The fresh tissue was minced into small pieces, digested with collagenase and filtered to obtain a single cell suspension, which was incubated with antibodies against cell surface markers specific to each of the 3 prostate epithelial cell types, and sorted into distinct epithelial cell populations by fluorescence-activated cell sorting. The cell types were confirmed by RT-PCR and western assays.
Results: 1. Tissue from 80 cases was procured, 41% of which had cancer.
2. A total of 0.5-5 x 10^6 viable cells/case were obtained.
3. Using 3 antibodies against cell surface markers, distinct populations of epithelial cells were identified and sorted. Basal (Trop2^{high}CD49f^{high}), luminal (Trop2^{high}CD49f^{low}) and neuroendocrine (CD56^{high}) cells were isolated from benign prostate while malignant lumina-type tumor cells and neuroendorcrine cells were isolated from tumor.
4. The benign and malignant cells contain high quality RNA as determined by ND8000 and Agilent 2100.
5. The benign epithelial cells were infected with lentivrisues expressing oncogenes, combined with supportive stroma, and transplanted into immunodeficient mice. High grade PIN occured at 12 weeks and invasive prostate cancer occured at 16 weeks, confirming tha viability of the isolated cells.
Conclusions: 1. We have developed a robust protocol to procure fresh human prostate tissue to obtain live benign and malignant epithelial cells
2. A combination of 3 antibodies separates prostate epithelial cells into distinct populations
3. The cells prepared are viable and can be used for biochemical and molecular studies as well as animal experiments, which will be invaluable in studying the molecular mechanisms directly applicable to human cancer.

1927 Developing a Digital Analysis Algorithm To Count Intraepithelial Eosinophils on H&E Stained Sections for Diagnosis of Eosinophilic Esophagitis.
V Parimi, A Zago, XJ Yang, ZE Chen. Northwestern University, Chicago, IL.
Background: Eosinophilic Esophagitis (EoE) is a distinct clinicopathologic entity with classic symptoms and endoscopic findings. Histologically, it is characterized by increased infiltration of eosinophils in the esophageal squamous mucosa. Quantification of intraepithelial eosinophil is a major diagnostic criterion. Manual enumeration has been shown not only tedious but also inconsistent among observers. We attempt to develop an automated counting algorithm using Aperio Genie program.
Design: Five H&E stained slides of esophageal biopsies from EoE patients were selected and scanned at 20X objective with Aperio Scanscope automated digital scanner. An automated counting algorithm was developed by training Aperio Genie program to recognize characteristic features of eosinophil cytoplasm and nuclear size. To validate the accuracy, the algorithm was applied to selected fields of the digitally scanned slides. In each field, computer generated positive events were visually located and compared to the corresponding H&E image. False positive and negative events were identified and a concordance rate was calculated by dividing the number of computer generated correct events to the number of visually identified eosinophils.
Results: After testing multiple settings, we developed an optimal algorithm incorporates both features of eosinophilic granular cytoplasm and nuclear size exclusion criteria as classifiers. This algorithm was applied to 21 selected areas covering all five scanned H&E sections. The concordance rate ranged from 57% to 100%, with a mean of 84$\pm$14 %. False positivity was primarily due to red blood cells contamination and eosin staining artifact at the edge of tissue fragments. Overall false negativity was 9.7% and was mainly due to less well revealed eosinophil cytoplasm. By eliminating these factors, the concordance rate reached to 100% in all 5 additional tested fields.
Conclusions: We have demonstrated the feasibility for developing an algorithm for automated enumeration of eosinophil on H&E slides with great accuracy. This is potentially useful for standardization of EoE diagnosis and research.

1928 Diagnostic Testing for *IDH1* and *IDH2* Variants in Acute Myeloid Leukemia: An Analgorithmic Approach Using High Resolution Melting Curve Analysis.
KP Patel, BA Barkoh, Z Chen, D Ma, LJ Medeiros, R Luthra. The University of Texas M.D. Anderson Cancer Center, Houston.
Background: Mutations at R132 of *IDH1* and at R140 and R172 of *IDH2 and*, polymorphism in G105 of *IDH1* are clinically significant in acute myeloid leukemia (AML).The frequency of these mutations in AML is 5-15%. The widely used labor intensive Sanger sequencing method is impractical for routine detection of such low frequency mutations in clinical laboratories. Alternative reported methods such as pyrosequencing, high resolution melting (HRM) curve and restriction enzyme digestion

assays detect only *IDH1R132* and *IDH2R172*. Therefore, there is a need to develop screening assays that detect all four clinically significant variants including the G105 polymorphism in *IDH1*.
Design: We developed two clinical assays using HRM to screen all four variants i.e., G105 and R132 in *IDH1* and, R140 and R172 in *IDH2*. An M13 sequence was incorporated in to PCR primers to allow direct Sanger sequencing of the amplicons using the same set of M13 primers for all four variants following HRM analysis. The *IDH1* assay was optimized using the HT1080 cell line containing homozygous G105 polymorphism and heterozygous R132C mutation. Since no cell line containing *IDH2* mutations was available, patient samples showing *IDH2R140* or *IDH2R172* mutations were used to optimize *IDH2* assay. The OCI-AML3 Cell line was used as a negative control. We compared the results of the HRM assays with Sanger sequencing in 146 AML bone marrow samples.
Results: We observed a high concordance for all positive and negative results for *IDH1* (98%) and *IDH2* (94%) between the HRM assay and Sanger sequencing. Significantly, there were no false negative results by HRM. Table 1 shows the distribution of all mutant, wild-type and indeterminate calls by HRM and Sanger sequencing. The sensitivity of the assays in serial dilution studies using patient DNA was 7.9% for *IDH1* assay and 7.3% for *IDH2* assay.

Correlation between HRM and Sanger sequencing for the detection of *IDH1* and *IDH2* variants

		HRM Analysis					
		IDH1			*IDH2*		
		SNP/MUT	WT	Indeterminate	MUT	WT	Indeterminate
Sanger Sequencing	SNP/MUT	49	0	0	43	0	0
	WT	0	93	3	1	93	9

Indeterminate, HRM call where one of the two replicates is called wild type and the other is called variant; MUT, mutant; SNP, single nucleotide polymorphism; WT, wild type

Conclusions: The HRM assays described here are convenient and versatile assays that allow effective strategy for screening followed by confirmation by sequencing of alterations in G105 and R132 in *IDH1* and, R140 and R172 in *IDH2* in AML in routine clinical diagnostics.

1929 The Use of Direct Smears for Molecular and Immunohistochemical Studies on Cytologic Specimens: A Paradigm Shift for Cytopathologic Technique.
JB Placido, MH Roh, BL Betz, L Schmidt, SM Knoepp. University of Michigan, Ann Arbor.
Background: As the number of molecular diagnostic and prognostic tests applied to patient specimens continues to grow, it is of paramount importance for cytopathologists to optimize the triage of scarce material obtained from fine needle aspiration biopsies (FNABs). While cell blocks have traditionally served as the mainstay for molecular and immunohistochemical studies performed on FNABs, direct smears serve as a potentially abundant source of material for these ancillary studies.
Design: We first performed a survey of the cellularity of 76 consecutive routine cell blocks prepared from endobronchial ultrasound (EBUS) guided (FNABs) diagnosed as malignant. We next developed and optimized a procedure for fixation and immunocytochemistry on unstained direct smears prepared from FNABs of malignancies. Unstained slides were also optimized for fluorescence in situ hybridization (FISH). Finally, we optimized extraction of DNA for mutational analysis on Diff-Quik stained cytologic smears after verification of tumor cellularity and purity.
Results: Forty-three (57%) of 76 cell blocks from EBUS-guided FNABs of malignancies were either very sparsely cellular or acellular. Next, immunocytochemistry was performed on 52 unstained direct smears from malignant cytologic specimens utilizing the Ventana autostainer after brief formalin fixation and antigen retrieval. The cases included pulmonary squamous cell carcinoma (n=15), pulmonary adenocarcinoma (n=27), metastatic melanoma (n=6), and Hodgkin lymphoma (n=4); antibodies directed against TTF-1, Napsin A, p63, S-100, Mart1, Melan-A, HMB-45, CD15, and CD30 were utilized. Furthermore, DNA extraction from Diff-Quik stained smears of pulmonary adenocarcinoma for EGFR and KRAS mutation was successful in all performed cases (n=33). Activating mutations for EGFR were found in 3/33 cases, and KRAS was mutated in 11/33 cases. Finally, FISH for EWS rearrangement utilizing unstained direct smears was performed on two cases of Ewing sarcoma.
Conclusions: The immediate triaging of cellular material during the time of FNAB for successful immunocytochemical and molecular studies represents a major advance in diagnostic cytopathology. The ability to guarantee that sufficient material is present for ancillary studies, during on-site assessment, represents a paradigm shift for cytopathologic workup. It is anticipated that these methods will become the standard of care as increasing demands are placed on cytopathologists to render additional molecular diagnostic and prognostic information on routine cytology specimens.

1930 Does p16 Immunostain Discriminate between Low-Risk and High-Risk Human Papilloma Virus Infection?
*TM Primeaux, J Thomas.* LSUHSC-Shreveport, LA.
Background: p16, a cyclin-dependent kinase inhibitor and G1/S-phase cell cycle checkpoint regulator is often used as a marker of HPV and is an E7-mediated functional inactivator of retinoblastoma protein (pRB). The loss of pRB function leads to over-expression of p16 protein due to lack of negative feedback. E7 protein from HR-HPV is considered more effective in the inactivation of pRB compared to that of LR-HPV, hence the use of p16 as a surrogate marker of HR-HPV. This study aims to assess the efficacy of p16 staining to discriminate between HR-HPV and LR-HPV.
Design: 47 consecutive tissue biopies with HPV-ISH studies done within the last year were reviewed. All had 5-µm sections cut and stained with p16 antibody. p16 staining intensity and patterns were scored semi-quantitatively and correlated with the HPV-ISH results.

Results: Table 1 shows the HPV-ISH status and p16 staining correlation with tumor types. The LR-HPV HNSCC case was also HR-HPV+. Two laryngeal papillomas (LP), in addition to positive staining for LR-HPV, had focal HR-HPV positivity. The LP showed weak basal layer, membranous and scattered isolated p16+ epithelial cells, which was distinct from the full-thickness, intense, diffuse cytoplasmic and nuclear staining in HR-HPV+ tumors (Figures 1&2).

Table 1

Diagnosis	# of cases	LR-HPV DNA	HR-HPV DNA	p16	Incomplete Data
HNSCC	37	1	12	16	5
Laryngeal papilloma	6	4	2 (focal)	4 (focal)	0
Anal SCC	3	0	3	3	0
Perianal condyloma	1	1	1	0	0
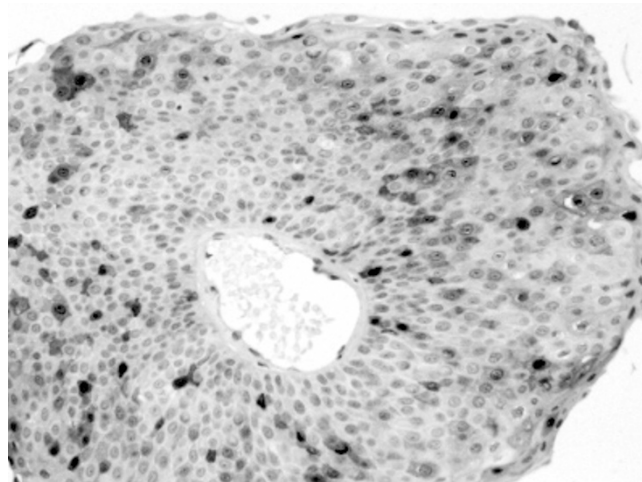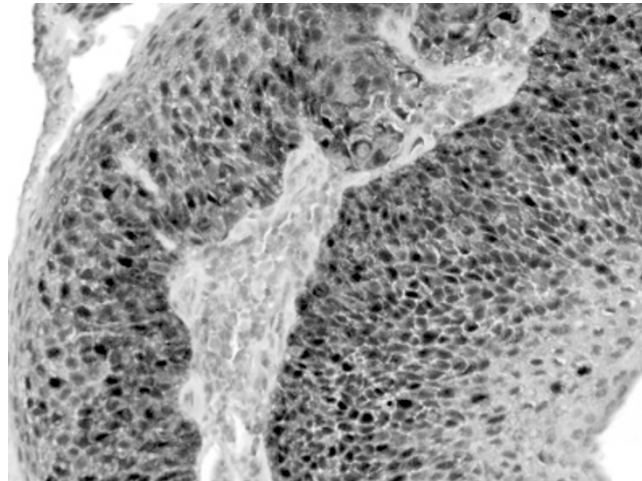
Conclusions: HR-HPV+ tumors show full-thickness, diffuse strong positive nuclear and cytoplasmic staining of cell clusters. Reactive LR-HPV tumors show only focal weak basal layer staining and scattered single cell positivity. Therefore, p16 IHC can distinguish between LR-HPV and HR-HPV infection in tumors with intense, diffuse staining pattern seen in HR-HPV+. These patterns must be taken into consideration when interpreting positivity to effectively distinguish between LR-HPV and HR-HPV infection.

1931 Meaningful Implementation of Computerized Speech Recognition (CSR) in Routine Pathology Reporting Must Be Determined by Its Accuracy and Efficacy.

Z Qu, C Jose, M Huynh, B Forcione, U Sivagnanalingam, S Thomas, K Alexaner. William Beaumont Hospital, Royal Oak, MI; University of Rochester Medical Center, NY.

Background: Effective implementation of computerized speech recognition (CSR) has been hampered by the lack of assessment of its effectiveness and shortcomings. We previously presented preliminary results of our objective outcome measurement of CSR. As the final part of our study, we stratify the measurements, and based on the data, propose recommendation for adopting this technology in surgical pathology.

Design: Voice dictation of 2,873 routine surgical pathology cases was simultaneously captured by CSR and routine transcriptionist-assisted documentation (TAD). Five additional participants whose native language is English also used CSR to capture the accession numbers and patient names of these cases. Fifty-two diagnostic templates (including "Note" in some) representative of routinely encountered disease spectrum were repeated in CSR by the participants. The accuracy in each report component (table) by CSR was compared to those by TAD and/or the templates. Dragon Naturally Speaking (v9) by Nuance installed in Dell Precision desktop computers with Microsoft Window-XP was used for the CSR.

Results: The accuracy of CSR for different components in pathology report varies greatly. Highest accuracy rate for the main diagnosis components requires 5-8% reduction in dictation speed from that for TAD.

Table. Accuracy of Different Report Components by CSR

Report Component	N =	N of CSR Participant	Accuracy rate (%) *	Comment
Patient Name	2,873	6	31-46	
Accession Number	2,873	6	75-82	
Diagnosis	2,873	1	91.6-94.4	Dictation speed as that for TAD
	52	5	93.7-97.8	Dict.speed to maximize accuracy
Report Format	2,873	1	0.71-2.2	Format pre-defined in CSR
	52	5	4.5-7.9	No pre-defined format

* Accuracy range includes low and high ends. All data shows normal distribution. No statistical analysis is used for the data presented here.

Conclusions: Combing our studies, we conclude and recommend: 1) Accuracy rate of CSR for (accession) number and patient name are not acceptable for routine use. Thus, manual input or bar-code method should be used. 2) Formats should be pre-defined by software macro function for consistent report style. 3) Pre-defined diagnosis templates are the most efficient and accurate approach when using CSR. 4) Increased dictation time by pathologists using CRS to achieve acceptable accuracy may likely offset the financial benefit from reducing TAD. The ultimate financial outcome remains to be determined.

1932 Effect of Processing and Fixation Time on IHC Results for Breast Biomarkers.

S Quan, W Pierceall, M Wolfe, L Alaparthi, J Kutok, B Ward. On-Q-ity, Waltham, MA; Brigham and Women's Hospital, Boston, MA.

Background: IHC Biomarker expression levels of FFPE-derived sections have been reported to discriminate therapeutic response in a variety of solid tumor malignancies. While the field has generally employed subjective classification by trained pathologists using standard 1+, 2+, 3+ scoring strategies, advances in digital pathology and image analysis software offer the potential for more objective analysis using specific computer scoring algorithms. The goal of our development program is to create accurate cut-off values for prediction of therapeutic response. However, potential technical issues remain that may hinder correct placement of patients within a biomarker expression continuum. One potential obstacle may be the effect of variability in processing and fixation time on the protein expression assayed by IHC as scored by digital pathology systems.

Design: To investigate the magnitude of this potential obstacle, we collected breast resection tumor samples from 6 individual patients and divided these tumors into 6 aliquots. Each aliquot was immediately fixed in 10% neutral buffered formalin for 2, 8 or 48 hrs, or was held overnight after at 4°C in saline before fixing. Sections were stained with three biomarkers using optimized automated protocols. Tumor regions were annotated and scored with user defined macros. Variation in staining quantity and intensity, defined by a multiplicative formula for computer generated values, were compared between the various processing and fixation times.

Results: BRCA1, XPF and ATM nuclear localized IHC signal was assessed and the scores derived did vary with fixation time and temperature. Increasing fixation time from 2 to 48 hours enhanced the ability to detect antigen. The variation was not uniform across all markers as BRCA1 was shown to be the most variable with scores from digital pathology analysis within individual patients ranging from 0 to 275 (scale 0-300). While ATM and XPF showed less dramatic variation among fixation conditions, enhanced antigen detection was a consistent trend with the longer fixation of 48 hrs.

Conclusions: In contrast to previous studies on the expression of ER and PR, the DNA repair nuclear localized proteins examined in this study display substantial variation in macro-derived scores due to fixation. These data indicate that uniform fixation will eliminate one source of variation for IHC results, and is a necessary precursor to proper patient placement in studies designed to develop diagnostic algorithms to identify chemotherapy responders and non-responders with high sensitivity and specificity.

1933 Is Virtual Microscopy Ready for the Prime Time? A Comparison with Conventional Microscopy.

C Reyes, F Ikpatt, M Nadji, RJ Cote. University of Miami Jackson Memorial Hospital and Sylvester Cancer Center, FL.

Background: Automated whole slide imaging, also known as virtual microscopy (VM) is rapidly becoming an important tool in diagnostic pathology. Currently, the major utility of VM is for transmission of digital images for consultations and second opinions. The high resolution of images and refinement of technology now allows for VM to be used as an alternative to conventional microscopy (CM), as a first line diagnostic platform. We investigated that possibility by comparing the histologic diagnoses of breast biopsies by CM and VM.

Design: One hundred and three needle biopsies of breast were randomly selected for this study. Each slide was scanned at 20X by BioImagene iScan Coreo Au. Three board-certified pathologists with varying degrees of experience in breast pathology independently reviewed the glass slides by CM, VM and again by CM during periods of one week intervals. Diagnostic categories included fibrocystic disease with or without ductal hyperplasia (DH), atypical ductal hyperplasia (ADH), ductal carcinoma in situ (DCIS) and invasive ductal carcinoma (IDC). The intra-pathologist reproducibility was recorded for CM vs VM and for CM vs CM, as control of the baseline. In those cases with inter-pathologist disagreement, the three observers jointly reviewed the glass slides by CM and agreed on a final diagnosis.

Results: Of the 103 core needle biopsies, 46 were malignant (22 DCIS, 24 IDC), 6 ADH and 51 fibrocystic disease (11 with DH). The intra-observer variability for CM vs VM was1% (observer 1), 4% (observer 2), and 1% (observer 3). The intra-observer variability for CM vs CM was 4%, 7% and 0% for observers 1, 2 and 3 respectively. All diagnostic disagreements were between DH and ADH. There were no intra- or

inter-observer disagreement in the diagnosis of benign vs malignant disease.
Conclusions: Virtual microscopy using high resolution whole slide images compares favorably with conventional microscopy for the first line diagnosis of breast biopsies.

1934 Lymphocyte Subset Reference Ranges for Evaluation of Immune Reconstitution after Allogeneic Stem Cell Transplantation.

BC Schur, AM Harrington, SH Kroft, H Olteanu. Medical College of Wisconsin, Milwaukee; Dynacare Laboratories, Milwaukee.

Background: Allogeneic stem cell transplantation (SCT) has become a common procedure for treating hematologic malignancies. Unfortunately, cure is often hampered by relapse of underlying disease, graft-versus-host disease, or severe opportunistic infections, which account for the majority of deaths after SCT. Therefore, it is important to evaluate the reconstitution of different immune cell subsets after SCT. Since there is only limited literature data on suitable reference ranges, we conducted a large study to establish comprehensive reference ranges for peripheral blood (PB) lymphocyte subsets useful in monitoring immune reconstitution after SCT.

Design: PB specimens from 76 healthy volunteers were run on an Advia 2120 hematology analyzer to determine white blood cell and absolute lymphocyte counts. Flow cytometry was performed on a FACSCanto II instrument, with the following antibodies: CD45RA/CD8/CD3/CD4/CD45, CD3/CD16+56/CD20/CD45, and HLA-DR/CD25/CD3/CD45. Boolean gates and quadrant markers were employed to record the following lymphocyte subsets: CD3+CD4+, CD3+CD8+, total CD3+, CD4/CD8 ratio, CD4+CD45RA+, total CD45RA+, CD(16+56)+CD3-, total CD19, total CD20, CD3+CD25+, CD3+HLA-DR+, CD25+HLA-DR+, total CD25+ and total HLA-DR. Statistical analysis was performed with EP Evaluator (Data Innovations, South Burlington, VT).

Results: There were 23 men and 53 women (mean age=37 years). The median white blood cell and absolute lymphocyte counts were: 6550/ul and 2065/ul. Study ranges for CD3+CD4+, CD3+CD8+, total CD3+, CD4/CD8 ratio, CD(16+56)+CD3-, total CD19, and total CD20 agreed with published data. Mean and standard deviation (SD) were calculated for the remaining subsets and ± 2SD ranges are shown in Table 1.

Table 1.

Subset	Mean	Mean±2SD
%CD4+CD45RA+	22.3	9-36
absolute CD4+CD45RA+/µL	456.4	145-768
total %CD45RA+	62.0	43-81
total absolute CD45RA+/µL	1268.7	691-1846
%CD3+CD25+	28.5	13-44
absolute CD3+CD25+/µL	576.7	217-936
%CD3+HLA-DR+	8.7	1-16
absolute CD3+HLA-DR+/µL	176.4	13-340
%CD25+HLA-DR+	3.0	1-5
absolute CD25+HLA-DR+/µL	60.4	14-107
total %CD25+	33.8	17-50
total absolute CD25+/µL	687.6	276-1099
total %HLA-DR+	22.8	11-34
total absolute HLA-DR+/µL	460.9	198-724

Conclusions: Our results are similar to those published for some of the lymphocyte subsets. Furthermore, we establish a comprehensive collection of clinical reference ranges in a large multiracial cohort, reflective of the general population. This data can be used for effective monitoring of immune reconstitution after SCT.

1935 Is the Anti-S-100 Antibody Decreasing Its Affinity for Epidermal Melanocytes? A Possible Diagnostic Pitfall.

FJ Solano, J Kapil, MT Deavers, MS McLemore, VG Prieto. University of Texas Health Science Center at San Antonio; George Washington University Medical Center, Washington, DC; University of Texas M.D. Anderson Cancer Center, Houston.

Background: Immunohistochemical (IHC) staining with anti-S-100 is used as a reliable marker of melanocytic differentiation. At MD Anderson Cancer Center (MDACC), IHC technique employs a monoclonal antibody derived from murine species stimulated with the purified bovine S-100 protein immunogen (clone 15E2E2), used in a 1:900 dilution to stain paraffin-embedded tissue following a standard protocol. Based on our experience at MDACC, anti-S-100 IHC frequently fails to label epidermal melanocytes while strongly labeling epidermal and dermal dendritic cells and nerves. Our objective is to determine whether epidermal melanocytic staining affinity with anti-S-100 is preserved in dermatopathology cases.

Design: We searched the Pathology files at MDACC for recent inside and outside consultation cases in dermatopathology in which anti-S-100 IHC was performed and available for review. Epidermal melanocytes labeling with anti-S100 were evaluated in each case for intensity (0: negative, 1: weak, 2: moderate to marked), and for percentage of cells staining (0: negative, 1: 1-25%, 2: 26-75%, 3: >75 %). For one outside case, anti-S-100 IHC was repeated, and for another, the anti-S-100 was performed in-house.

Results: From 3/1/2010 to 9/24/2010, 28 skin cases (18 inside, 10 outside cases) were identified (see Table 1). All cases had squamous epithelium with normal melanocytes, as well as dermal dendritic cells and nerves to serve as an internal positive control. In a majority of cases, additional IHC had previously been performed which highlighted melanocytes (i.e., anti-MART1, HMB45, anti-tyrosinase, or MITF).

Table1: Intensity and Percentage of Anti-S-100 IHC Staining in Both Inside and Outside Skin Cases at MDACC

Intensity/Percentage of Staining with Anti-S-100:	0/0	1/1	2/1	1/2	2/2	2/3
Number of Inside Cases:	4	9	2	1	3	1
Number of Outside Cases:	1	4	0	1	1	2

Conclusions: This study suggests that current antibodies and IHC techniques employed to detect S-100 expression may have a relatively lower sensitivity for melanocytes

than other cells (e.g., Langerhans cells, nerves). When analyzing anti-S100 IHC, it is necessary to determine if the internal control melanocytes, when available, are labeled before considering that the slide is appropriate for interpretation.
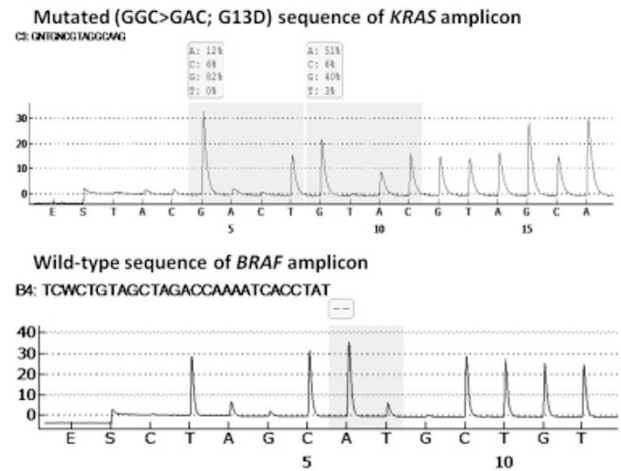
1936 *KRAS* and *BRAF* Mutation Detection with Multiplex Amplification and Pyrosequencing.

H Takei, M Szanyi, F Monzon. The Methodist Hospital, Houston, TX.

Background: Targeted therapies against receptor tyrosine kinase signaling cascades have revolutionized cancer treatment. For metastatic colorectal carcinomas (mCRCs), anti-epidermal growth factor receptor (EGFR) humanized monoclonal antibodies have been shown to improve patient outcomes. However, codon 12/13 mutations in the *KRAS* gene are associated with resistance to this novel targeted therapy. In addition, mutations in the *BRAF* gene, a downstream target of the same signaling cascade, have also been shown to confer resistance to anti-EGFR therapy. It is thus desirable to test for both *KRAS* and *BRAF* mutations, ideally as a multiplex assay. The aim of study is to design an assay using a multiplex PCR method for both *KRAS* and *BRAF* mutations and sequential pyrosequencing on the same amplification reaction.

Design: We designed a multiplex COLD-PCR protocol to amplify segments containing codons 12/13 of the *KRAS* gene and codon 600 of the *BRAF* gene. The PCR products were electrophoretically separated to confirm amplicon size. Pyrosequencing to detect *KRAS* and *BRAF* amplicon sequences were performed with sequencing primers specific to each gene. A *KRAS* mutant cell line (HCT116) and a wild-type control (placental DNA) were tested simultaneously.

Results: The electropherogram showed well-resolved peaks at 89 and 219 base pairs, corresponding to *KRAS* and *BRAF* amplicons respectively, in both specimens. Pyrosequencing demonstrated mutated (GGC>GAC; G13D) and wild-type sequences of *KRAS* amplicons, with wild-type sequence of *BRAF* amplicon, in the *KRAS* mutant cell line and the control DNAs, respectively. However, peak intensity in the sequencing reaction was reduced, and noise increased when compared to non-multiplexed PCR reactions.

Conclusions: We have demonstrated that both *KRAS* and *BRAF* mutations can be tested sequentially on the same multiplex amplification reaction with our assay design. Optimization of the assay and validation with a large number of samples will be performed before possible clinical implementation of this assay. These preliminary results suggest that this protocol should streamline KRAS/BRAF mutation testing by using a single amplification reaction to sequence both genes.

1937 Detection of HPV16 in Cervical Carcinoma Using Fully Automated In Situ PCR System.

S Thakur, S Mysore, S Guddu, AR Poongothai, H Wang, K Kalra. BioGenex, Hyderabad, AP, India; BioGenex, San Ramon, CA.

Background: Molecular detection of Human Papilloma Virus (HPV) DNA is currently the gold standard for detection of HPV. Various methods that are in use include, dot blotting, southern blotting, ISH, CISH, hybrid capture and PCR. Unlike conventional methods like PCR, *in situ* PCR (ISP) can help in detection of low copy nucleic acid targets (DNA/ mRNA) while preserving the histological context. In this study, we have reported the use of fully automated detection of HPV16 in cervical carcinoma tissue using ISP and established concordance between ISP and CISH.

Design: Cohort of 20 cervical carcinoma samples is used for the study. SiHa cell lines (1-2 copies of HPV16) have served as experimental control. Tissues from human breast, colon carcinoma and normal cervix are also tested. PCR primers are designed to amplify the E6 region of HPV16. Fluorescein labeled dUTP's are incorporated during PCR amplification and subsequently, amplicons are detected with sequential addition of anti-fluorescein antibody, and a poly-HRP labeled secondary antibody followed by final color development with DAB chromogen. HPV16 CISH is performed using single oligo-probe labeled with penta-fluorescein at 5' end. We have used Xmatrx®- a fully automated walk-away staining system to perform the complete assay.

Results: In this study, we are reporting for the first time successful detection of HPV16 using fully automated *in situ* PCR followed by chromogenic detection. The sensitivity of this detection is found to be as low as 1-2 copies of HPV16 using SiHa cell lines. All the 20 cervical carcinoma samples in this cohort detected positive for HPV16 by ISP and 15/20 are found to be positive by CISH. The results showed 75% of concordance

between HPV16 ISP and HPV16 CISH using automated detection system. Further, there is no HPV16 signal detected from breast, colon carcinoma and normal cervix tissues.
Conclusions: Fully automated ISP detection is observed to be 25% more sensitive when compared to CISH with an ability to detect even 1-2 copies of HPV16 using SiHa cell lines. Fully automated ISP offers rapid and sensitive method for histological localization of HPV. Further, this is useful for the early screening of HPV infection in cervical scrapings and cervical intraepithelial neoplasia, where early detection of very small quantities of HPV is critical for prediction of clinical outcome.

1938 Mapping Molecular Alterations in Breast Cancer Using Mammary Ductoscopy.

D Tran-Thanh, D-Y Wang, V Iakovlev, C Wang, JC Moreno, S Boerner, N Miller, B Youngson, WL Leong, SJ Done. CHUM Hotel-Dieu, Montreal, QC, Canada; Campbell Family Institute for Breast Cancer Researcn, Toronto, ON, Canada; University Health Network, Toronto, ON, Canada; University of Toronto, ON, Canada.

Background: Mammary ductoscopy is a new endoscopic technique that has the potential to allow direct visualization and sampling of tumor-containing mammary ducts. We are taking advantage this new technique to obtain epithelial cells at different intervals along these ducts. This will allow us to define a geographic map of the genetic alterations leading to malignancy in breast cancer.
Design: A series of women undergoing mastectomy for invasive breast cancer were subjected intraoperatively to mammary ductoscopy to identify the duct leading to the tumor and obtain cytology samples. Immediately after removal of the breast, a set of snap-frozen tissue samples were harvested along the identified duct as well as from the tumor itself. Nucleic acids were extracted from all cytological and microdissected tissue samples and subjected to array CGH and gene expression array profiling.
Results: Twenty-one patients undergoing mastectomy have been recruited in our study. Array CGH and gene expression data showed an increasing number of genetic alterations in epithelial ductal cells going from the nipple towards the tumor. Furthermore, in a small number of patients, genetic abnormalities similar those found in tumors can be identified in histologically normal ducts sampled close to the tumor. These include alterations to chromosomes 1q12-21, 8q21-24, 17q12-21 and 20q13.2, and might represent the earliest molecular changes leading to breast cancer. In addition, pathway analysis using gene expression data obtained from different regions of the affected duct demonstrated that certain pathways, notably the E2F1 and β-catenin pathways, were altered early on during tumorigenesis. On the other hand, activation of pathways such as PI3K or IFN-γ seemed to be occurring later.
Conclusions: Mammary ductoscopy is a useful technique for mapping molecular alterations in breast cancer patients. Using microarray data, we have identified chromosomal regions that might represent the earliest changes and pathways that seem to be activated early on during breast cancer development. Identification of some of the earliest events in tumourigenesis may result in new strategies to block the development and progression of breast cancer.

1939 RNA Quantity and Quality from Paraffin Blocks: A Comparison of Fixation, Processing and Nucleic Acid Extraction Techniques.

G Turashvili, W Yang, S Yip, M Carrier, N Gale, Y Ng, K Chow, L Bell, M Luk, S Kalloger, B Gilks, S Aparicio, D Huntsman. BC Cancer Agency, Provincial Health Services Authority, Vancouver, BC, Canada; Vancouver General Hospital and University of British Columbia, BC, Canada.

Background: RNA extracted from paraffin blocks can be used for clinical molecular diagnostic assays, including RT-PCR, quantitative PCR, cDNA library construction and most recently whole transcriptome shotgun sequencing. Although the capacity to extract high quality RNA from paraffin blocks is crucial, there is little information available to guide laboratories in their selection of tissue fixation, processing and RNA extraction techniques.
Design: Nine human tissue samples (three each of colon, liver and muscle) were subjected to the following fixation and processing conditions: (1) flash freezing; (2) neutral buffered formalin (NBF) fixation <24 hours (NBF24); (3) NBF fixation 7 days (NBF7); (4) molecular fixative (MF) <24 hours; (5) MF 7 days. NBF-fixed samples were processed by standard processing (Tissue-Tek VIP5 processor, Somagen, Canada), and MF-fixed samples by rapid processing (Tissue-Tek Xpress, Somagen). Total RNA was extracted using phenol-chloroform manual extraction, RecoverAll (Ambion, USA), Waxfree RNA (Trimgen, USA), and RNeasy FFPE Kit (Qiagen, Canada). RNA was quantified using a Nanodrop spectrophotometer, and one-step RT-PCR was used for the amplification of two ACTB fragments (621 bp and 816 bp).
Results: Manual extraction and WaxFree RNA kit yielded higher amounts of RNA when compared with RNeasy and RecoverAll kits, independent of the type of tissue, fixation or processing. For frozen tissues, there was no difference between manual extraction and WaxFree RNA kit for 621 bp amplicon but manual extraction performed better for 816 bp amplicon (p<0.001). In MF-fixed tissues, both amplicons were successfully amplified using all extraction methods except for WaxFree RNA kit. For NBF24 tissues, 621 bp amplicon was amplified using all kits but manual extraction performed better for the 816 bp amplicon (p<0.001). For NBF7-fixed tissues, manual extraction and WaxFree RNA kit were superior to RNeasy and RecoverAll kits (p<0.01). None of the extraction kits succeeded in amplifying the 816 bp amplicon in a majority of NBF7 samples.
**Conclusions:** The molecular fixative, regardless of the duration of fixation, and the rapid processing system used in this study were able to preserve RNA in paraffin blocks with successful RT-PCR for as long as 816 bp amplicons, making these techniques suitable for use in downstream molecular diagnostic assays.

1940 Pouring Stabilization Bodies for Paraffin Tissue Microarrays Using Agar and Top Pin Tissue Arrayers.

UF Vogel. University Hospital, Eberhard-Karls-University, Tuebingen, Baden-Wuerttemberg, Germany.

Background: Paraffin tissue microarrays (PTMAs) are a well-accepted technique especially in translational pathology. Up to 2500 paraffin tissue core biopsies (PTCBs) can be installed in preformed holes in so-called recipient paraffin blocks (37 x 23 x 5 mm). To prevent the rolling and folding of PTCBs at sectioning a melting process of the filled PTMAs is recommended. However, the PTCBs may topple down during the melting process if more than one PTCB (composite PTCB) is installed in one hole of the PTMA. This problem can be solved by using so-called stabilization bodies, i.e. paraffinized agar plates (35 x 21 x 4 mm) with preformed holes. The present study should investigate whether the construction of low cost agar stabilization bodies can be easily feasible by using top pin arrayers.
Design: A boiling 2% agar solution was poured into different molds (e.g. plastic lid of a pipette tip box). Top pin arrayers (Figure 1A) were placed from above into the hot and liquid agar (Figure 1B). After solidification the pins were withdrawn resulting in agar plates with preformed recipient holes (Figure 1C). These agar plates were paraffinized in an ordinary tissue processor. The paraffinized agar plates (Figure 1D) were embedded in paraffin blocks (Figure 1E) or used as stand alones. The PTMAs were filled manually with PTCBs (Figure 1E) in a routine fashion and then completely melted (30 minutes, 60°C). After resolidification the PTMAs were cut and the sections stained according to standard procedures.
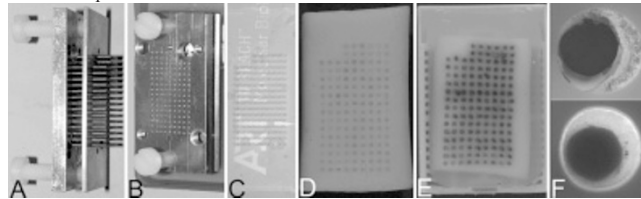
Results: It was easily feasible to pour the holes of the agar stabilization bodies using top pin arrayers. Paraffinization of these agar plates was successfully done using ordinary tissue processors. Prior to the melting process the PTCBs missed a strong contact to the surrounding paraffin (Figure 1F, top). The stabilization bodies prevented the PTCBs from toppling during the melting process. After the melting process the PTCBs firmly adhered to the surrounding paraffin and the paraffinized agar (Figure 1F, bottom).
Conclusions: The construction of low cost agar stabilization bodies is feasible using top pin arrayers. Agar stabilization bodies enhance the efficacy and quality of the PTMA technique by providing a melting procedure for composite PTCBs.

1941 Mid-Infrared Spectroscopic Imaging for Breast Tissue Histopathology: Towards 'Stainless Staining'.

MJ Walsh, DM Mayerich, EL Wiley, A Kajdacsy-Balla, R Bhargava. University of Illinois at Urbana-Champaign; University of Illinois Medical Center, Chicago.

Background: Mid-Infrared (IR) spectroscopic imaging is a novel approach to derive chemical images from tissues based on their inherent biochemistry. Histopathology is the gold standard for disease diagnosis. Current histopathological techniques use of panel of special stains and immunohistochemistry (IHC) to assess tissue architecture, determine cell types present and to classify cancers.
Design: Mid-IR images were obtained from over 200 individual patients using breast tissue microarrays. Serial sections were stained with a panel of 13 routinely used special stains and IHC stains. A modified Bayesian classifier was built to assign image pixels to the correct cell types and Artificial Neural Networks (ANN) to replicate staining.
Results: Using Mid-IR imaging coupled with the modified Bayesian classifier it was possible to segment breast tissue into the main 8-cell types of breast tissue from a single unstained tissue section. The sensitivity and specificity as measured by average Area Under the Curve (AUC) were very high (AUC=0.9). Mid-IR imaging coupled with ANN demonstrated that it was possible to accurately reproduce the staining of the panel of stains, all in a single unstained slide.
Conclusions: Mid-IR imaging coupled with Bayesian classification and ANN could potentially be a very valuable tool as an adjunct to current histopathological procedures, with the ability to take a single unstained tissue section and give a decision on the cell types present and also to replicate staining patterns. This approach could be particularly advantageous where limited histological and cytological specimen is available for analysis. Moreover, it is amenable to quantitative analysis of each component. This novel approach promises to revolutionize and expand the role of the pathologists in both research and tissue diagnosis.

1942 Mid-Infrared Spectroscopic Imaging as an Approach To Identify the Early Chemical Changes in Kidney Glomeruli Associated with Diabetes.

MJ Walsh, S Setty, A Kajdacsy-Balla, R Bhargava. University of Illinois at Urbana-Champaign; University of Illinois Medical Center, Chicago.

Background: The ability to detect the initial changes of diabetic and obesity-related glomerulopathy in tissue sections is limited. There are no tools to recognize biochemical changes in the glomerulus that could be applied to early diagnosis. Mid-Infrared (IR) spectroscopic imaging represents a novel approach to derive chemical images of kidney tissue based on the tissues biochemistry. Our group has made progress towards the development of high-resolution mid-infrared imaging towards basement membrane identification and chemical characterization in human tissues. In this study we examine the feasibility of using mid-infrared imaging to detect pre-diabetic and diabetic changes in glomeruli.

Design: Recent advances in high-resolution mid-infrared imaging has allowed for detailed chemical images of kidney glomeruli to be acquired. As a proof of principal we studied a representative number of normal, pre-diabetic and diabetic cases. Mid-IR images were acquired of normal, pre-diabetic, and diabetic kidney biopsies with paraffin-embedded tissue samples with H&E – stained serial sections. IR images were acquired at 1.56, 6.25 and 25-micron spatial resolution.

Results: Mid-IR imaging coupled with modified Bayesian classification could rapidly identify the presence and number of glomeruli within tissue biopsies, even at a coarse spatial resolution (25microns). More importantly, high resolution images of glomeruli (1.56microns) revealed differences in the chemical makeup of the basement membrane were that allowed distinguishing between normal, pre-diabetic and diabetic patients.

Conclusions: Due to the novel availability of high-resolution mid-IR imaging that allows visualization of basement membranes, it was possible for the first time to detect biochemical changes that precede light microscopy signs of diabetic glomerulopathy. This technique is promising since it could be used to predict progression of disease such as in patients after transplant for diabetic glomerulosclerosis.

1943 Detection of Herpes Simplex Virus 1,2: Comparison between In Situ Hybridization and Immunohistochemistry Methodologies.
FJ Walsh, BE McCann, KL Grogg. Mayo Clinic, Rochester, MN.
Background: Clinically, Herpes Simplex Virus 1,2 (HSV) testing is important to distinguish it from other types of skin lesions, as well as to identify HSV in infected organs when the virus disseminates to other parts of the body. In our practice, both the Immunohistochemistry (IHC) and the In Situ Hybridization (ISH) laboratories perform testing for HSV 1, 2 on tissue sections. In order to streamline processes between the labs and eliminate redundancy, the 2 test methods were compared.
Design: Testing was performed on formalin fixed-paraffin embedded (FFPE) tissue sections. A total of 58 cases were collected on which HSV testing either by ISH or by IHC had been previously performed. After heat induced epitope retrieval in EDTA pH 8.0, IHC testing was performed on a Dako Autostainer using a rabbit polyclonal antibody (Cell Marque), dilution 1:200, with Dako Advance detection and DAB chromagen. The ISH testing was performed using a manual procedure and a biotin labeled probe (Enzo Life Sciences Inc.) followed by streptavidin alkaline phosphatase detection (Vector) with NBT/BCIP chromagen (Roche). Completed slides were reviewed by two technologists and a pathologist.
Results: Of the 58 cases tested, 42 were positive by IHC showing strong staining of viral and cytoplasmic inclusions in infected cells. 40 of these cases were positive for HSV by ISH, showing primarily nuclear staining in infected cells. 2 additional cases showed equivocal positivity by IHC with staining in necrotic debris only, and were negative by ISH. Of the 4 cases that were positive or equivocal for HSV by IHC but negative by ISH, 3 were skin biopsies of vesicular lesions showing morphologic features suggestive of herpetic infection on H&E levels, and thus were considered a true positive result. The fourth case was a lung biopsy showing a lymphohistiocytic infiltrate with necrosis in an immunosuppressed patient. A nasal swab from this patient was positive for HSV1 by PCR studies, supporting the conclusion that the IHC staining in necrotic debris represented true positivity. Overall, our ISH method detected HSV in 91% of the cases that were positive by IHC.
Conclusions: For the detection of HSV 1,2 in FFPE specimens, our ISH and IHC methods give comparable results, with IHC showing slightly better sensitivity than ISH, particularly in necrotic tissues.


1944 Use of Image Analysis in Immunohistochemistry (IHC) Assay Development and Quality Control.
S Webster, C Roach, V Tanna, J Erickson, K Wakamiya. Dako North America, Inc., Carpinteria, CA.
Background: Image analysis is gaining increasing acceptance as a tool for the interpretation of IHC stains in the pathology laboratory. A number of slide scanners are now available that provide algorithms designed for the assessment of clinical markers such as HER2, ER/PR and Ki-67. In addition, such platforms can have utility beyond their primary duty of evaluating clinical specimens. For example, image analysis can provide benefit to activities such as assay development and daily quality control, thereby adding value across the spectrum of laboratory workflow.
Design: Activities typically performed in the development of IHC assays include titering the primary antibody, defining scoring approaches and establishing quality control methods. To illustrate the application of image analysis to such activities, an assay for ßIII-Tubulin (ß3T) IHC currently in development in our laboratory was used as an example. Stained slides were scanned using the ACIS® III and scored using an algorithm based on the intensity of the IHC stain. Where required, slides were manually scored in parallel using the H-score method (Budwit-Novotny et al., 1986, Cancer Res 46:5419-5425).
Results: Antibody titration. Intensities from slides stained using sequential titrations of different anti-ß3T batches were plotted against dilution factor. The resulting plots were used to calculate the dilutions required to obtain equivalent staining. These dilutions compared favorably to the IgG concentrations of the antibody batches ($p<0.05$). Scoring IHC stains. Image analysis results exhibited a significant correlation with manual assessment (H-score), demonstrating the ability to replicate complex manual scoring schema (r=0.79, $p<0.05$). Reproducibility/Quality control. As a model for tracking staining batch controls, tissue sections from 27 consecutive experiments (stained as part of precision studies) were scanned, their IHC intensities plotted in a Levey-Jennings style chart and evaluated using Westgard rules:
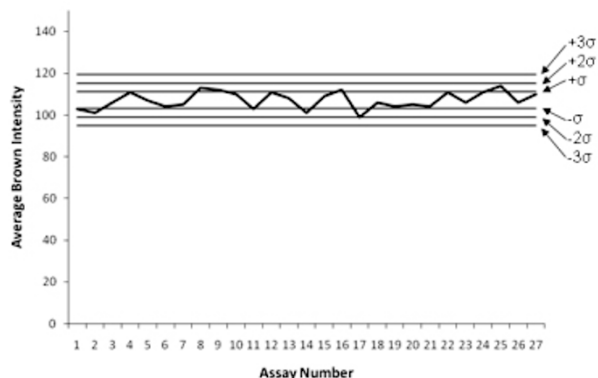
Conclusions: These results demonstrate the successful application of image analysis methods to laboratory activities above and beyond the primary use of assessing clinical specimens. This suggests additional value for the technology, particularly in laboratories that engage in development and/or QC activities.

1945 A Validation Study of Quantum Dot Multispectral Imaging To Evaluate Hormone Receptor Status in Breast Ductal Carcinoma In Situ (DCIS).
J Yu, SE Monaco, R Bhargava, DD Dabbs, KM Cieply, JL Fine. University of Pittsburgh Medical Center, PA.
Background: The assessment of hormone receptors, including estrogen receptor (ER) and progesterone receptor (PR), has become a standard practice in breast cancer management. Currently, the recommended method is conventional immunohistochemistry (IHC) to detect protein expression levels. However, there are problems associated with the receptor analysis by IHC. The quantitative analysis (e.g. 1% of cells with weak signal for ER/PR positive result) has been subjected to interobserver variations; the need for multiple sections to evaluate each receptor individually by single-stained IHC often preclude the analysis on core biopsies with limited amount of invasive tumor or with microinvasive carcinoma. A more objective and efficient method would be optimal for the detection and quantification of breast cancer receptors. The aim of the study is to validate the quantitative analysis of ER and PR by Quantum Dot (QD) based IHC using multispectral imaging (MSI).
Design: A total of 17 cases of breast ductal carcinoma in situ (DCIS) with excisional biopsies or mastectomies were stained with conventional IHC and QD based IHC for ER and PR. For conventional IHC, a semi-quantitative H-score, as well as corresponding percentage of positive cells, was calculated. For QD-based IHC, three regions of interest (ROIs) were selected and captured for each case at 20x magnification for single-labeled ER (585nm) and PR (655nm), in addition to double labeled ER/PR. DAPI was used as a nuclear counterstain. Co-localization data between ER or PR and DAPI was analyzed by CRI Nuance FX multispectral imaging system using software version 2.10.
Results: Co-localization ratios of ER/DAPI or PR/DAPI by double-labeled QD-based IHC were compared with those by single-labeled QD-based IHC as well as either the H-score or percentage of positive cells by conventional IHC. For ER stains, there was good consistency between double- and single-labeled QD-based IHC (r = 0.93, P < 0.001), and QD-based IHC correlated well with both H-score (r = 0.94, P < 0.001) and percentage of positive cells (r = 0.89, P < 0.001) by conventional IHC. The PR stains showed similar results.
Conclusions: The QD-based multiplex, multispectral technique is able to reliably detect and measure multiple co-localized biomarkers in the same cellular compartment, such as nuclear ER and PR, on single paraffin embedded tissue sections. This technique can enhance our ability to assess breast tumor markers in specimens with limited available tissue, especially as complex image analysis is better developed.

1946 Optimizaton of Fixation and Processing of Biopsy Gun Prostate Needle Biopsy Specimens.
RJ Zarbo, N Gupta, R Varney, N Main, S Richard, B Mahar, ON Kryvenko, S McMahon, N Draga, O Alassi, A Ormsby, R D'Angelo. Henry Ford Health System, Detroit, MI.
Background: Consistency of nuclear and cytologic detail in prostate needle biopsy specimens is a critical aspect of histopathologic diagnosis. The preanalytic parameters of formalin fixation from time of surgical procedure are largely uncontrolled and inadequate fixation may contribute to less than optimal histology when using same-day rapid tissue processing. To accomodate this unstandardized variable by defaulting to overnight fixation of Biopty gun prostate needle biopsies negates the advantage of rapid cycle processing.
Design: We performed Biopty Gun (Bard Peripherial Vascular, Inc. Tempe, AZ) needle biopsies of fresh clinical prostatectomy specimens to test 18 pathway variations of tissue fixation and processing. Needle (18G) cores obtained from the posterior aspect of glands (8 per side) were 1 mm or less diameter and averaged 15-18 mm length. To control for variation in fixation time and mimic air-drying, cores were placed on saline soaked gauze initially before testing combinations of no fixation other than on processors, timed tissue fixation at room temperature, desktop microwave formalin fixation for 3.5 minutes (Model EBS42850, Energy Beam Sciences, East Granby, CT), controlled heated fixation for 30 minutes at 37°, 45° and 50°C (FixMate, Milestone Medical Technologies, Inc, Kalamazoo, MI/Sirasole, Italy) and processing on two microwave enhanced instruments, Tissue-Tek Xpress (Sakura Finetek USA, Inc, Torrance, CA)

and Pathos DELTA (Milestone Medical Technologies). Quality assessments were made of ease of embedding and microtome sectioning and histopathologic variables of hematoxylin and eosin staining intensity, homogeneity, nuclear preservation, nucleolar prominence, autolysis or thermal artifact. Microscopic sections were evaluated by one GU pathologist. Microscopic quality was scored on a 10-part scale.

Results: With the exception of the FixMate heated and timed fixation tests at 37°C and 45°C, all combinations gave inconsistent and spotty unacceptable, suboptimal to good microscopic preparations no matter the variable manipulated. The higher 50°C test of heated formalin fixation resulted in an artifact of nuclear chromatin that was dark and smudgy. The histologic quality at 37°C was judged slightly superior to 45°C. No significant difference in quality of tissue microtomy or histologic preparation was noted for either microwave tissue processor.

Conclusions: Enhanced consistency in the quality of histologic preparations using rapid microwave processors is obtained when prostate needle biopsy fixation is standardized with controlled time and temperature of fixation.

1947 Integration of Microwave Technology To Reduce Fixation and Processing Time of Robotic Prostatectomy Specimens for Whole Mount Examination.
RJ Zarbo, R Varney, O Alassi, N Main, S Richard, R D'Angelo, B Mahar, D Lubensky, ON Kryvenko, A Ormsby, S McMahon, N Draga, N Gupta. Henry Ford Health System, Detroit, MI.

Background: Using the Lean tool of value stream mapping, we identified the preanalytic phase of processes from specimen receipt to tissue processing as the major source of time delay and non-value added effort in the value stream of whole mount prostatectomy evaluation.

Design: We targeted intact gland formalin fixation and tissue processing of whole mount (WM) sections. The initial condition consisted of 50-100ml formalin needle injection of intact robotic prostatectomies using a fine needle. Intact glands were then fixed overnight in 32 oz. formalin for avg. 15.8 hours. Glands were entirely sectioned at 4mm thickness and WM sections were fixed for 9 hrs. in macro-cassettes (LPC1000, Cancer Diagnostics Inc) and processed for 16.5 hrs. in a VIP 300E processor (Sakura Finetek USA, Inc, Torrance, CA). The redesigned condition retained formalin injection of glands that were then fixed intact in 32 oz. of formalin for 30 min. followed by microwave fixation in 32 oz. of formalin in a microwave processor (Model EBS42850, EBSciences, East Granby, CT) at 450W for 6 min. at 50C°. Glands over 50 grams were held for 15 additional min. in formalin at room temperature then microwaved again for 3.5 min. WM sections were then fixed in macro-cassettes for an additional 2 hrs. at room temperature. Total fixation time in the redesigned process was 2.53 hrs. WM sections were processed in 7 hrs. in macro-cassettes in a Pathos DELTA microwave processor (Milestone Medical Technologies, Inc, Kalamazoo, MI/Sirasole, Italy). Baselines were from 20 robotic prostatectomies. New conditions were tested on 5 autopsy and 10 clinical glands.The latter were parallel tested with WM slices from each gland in the VIP and Pathos DELTA processors. All microscopic sections were assessed by one GU pathologist.

Results: With process redesign fixation time was reduced by 90% from 24.8 to 2.53 hrs. Integrating microwave technology in tissue processing reduced processor time by 58% from 16.5 to 7 hrs. Overall, 32 hrs. of non-value added time waste was removed from the front end processes resulting in a 77% reduction from 41.3 to 9.5 hrs. Pathologic examination showed no significant variations in quality related to H&E staining, homogeneity, crust/edge effect, completeness of margins, nuclear preservation, autolysis or thermal artifact.

Conclusions: Lean process redesign targeting intact prostate gland fixation and integration of microwave technology in radical prostatectomy processing can be of great benefit in addressing total timeliness of pathologic reporting.

1948 Nottingham-Defined Mitotic Score: Comparison to Visual and Image Cytometric Phosphohistone H3 Labeling Indices and Correlation with Oncotype DX Recurrence Score.
B Zbytek, C Cohen, AJ Page, AL Adams. Emory University, Atlanta, GA.

Background: Prognosis of breast cancer patients has been determined traditionally by lymph node status, tumor size, and histologic grade. In recent years the Oncotype DX Recurrence Score (RS) assay has emerged as a costly adjunct prognostic tool. Markers of proliferation play a large role in determination of RS, and we have shown previously that immunohistochemical expression of proliferation markers Ki-67 and phosphohistone H3 (PPH3) correlates with RS. Our current goal is comparison of the hematoxylin-and-eosin (H&E) mitotic score, defined by the Nottingham grading system, to anti-PPH3 mitotic figure labeling assessed by both visual and automated image analysis and correlation of mitotic score results with RS.

Design: Estrogen receptor-positive breast carcinomas from 138 patients with Oncotype DX testing were selected. A representative H&E-stained tumor section was evaluated. Mitoses were counted per 10 HPF and tumors graded using the Nottingham criteria by one pathologist in accordance with CAP-recommended mitotic count cutoffs for a field diameter of 0.55 mm. An additional section was immunostained with PPH3 antibody (Dako). PPH3 mitotic scores were determined visually per 10 HPF and by the Automated Cellular Imaging System III (Dako) in 10 "hotspots". Statistical analysis was performed using univariate tests and Pearson's correlation coefficient.

Results: There was a significant association between H&E mitosis score and RS ($p<0.001$, $R=0.34$).

Mitotic score	Oncotype DX Recurrence Score		
	Low	Intermediate	High
1	65 (56%)	43 (37%)	9 (7%)
2	6 (32%)	4 (21%)	9 (47%)
3	0 (0)	1 (50%)	1 (50%)

RS associations with visual and automated PPH3 mitotic scores were also significant (visual: $p<0.001$, $R=0.32$; automated: $p<0.005$, $R=0.25$). The three methods of mitotic score assessment were strongly associated with each other.

Method	Pearson's R	p
Mitotic Score: H&E vs. PPH3 Visual	.41	<0.001
Mitotic Score: PPH3 Visual vs. Automated PPH3	.71	<0.001
Tumor Grade Using H&E Mitotic Score vs. PPH3 Visual	.81	<0.001

Conclusions: The Nottingham-derived H&E mitotic score is significantly associated with RS. There is significant correlation between mitotic scores determined by H&E and by PPH3 labeling assessed visually and by imaging. There is significant correlation between grades determined by H&E and PPH3 labeling. Mitotic score by any of the three methods studied may be useful in assessing tumor grade, proliferation,and prognosis.
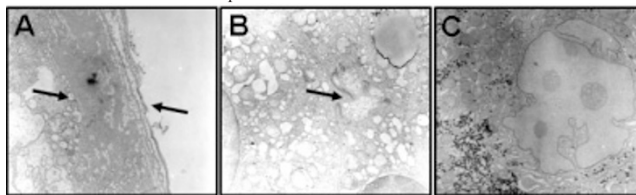
Ultrastructural

1949 Unique Ultrastructural Features in Diagnosis of Hepatocellular Carcinoma in Fine Needle Aspiration Cytology Specimen.
A Abdul-Nabi, G Sidhu, N Cassai, J Liao, G-Y Yang. Northwestern University, Chicago, IL; NYU School of Medicine, NewYork, NY.

Background: Fine needle aspiration cytology (FNAC) has been widely used as a minimally invasive and rapid method of diagnosis of primary or metastatic hepatic masses. But its sensitivity appears low (67% to 93%) and a negative result does not exclude malignancy. Although immunohistochemistry is commonly used as an ancillary test, definitive biomarker for hepatocellular carcinoma (HCC) is lacking. Many studies have shown that electron microscopy (EM) has the precise ability in identifying normal and neoplastic hepatocyte ultrastructurally, but its use is still limited. Our study aims to characterize unique ultrastructural features of HCC and evaluate its usefulness as a diagnostic tool in FNAC.

Design: FNAC specimens from 67 cases of HCC with different degrees of differentiation confirmed histopathologically by core-needle biopsy or hepatoectomy were collected between 1993-2003. Parallel FNAC specimens were submitted for EM examination.

Results: Among 67 HCC cases, 95% (64/67) of the cases was confirmed the FNAC diagnosis of HCC. In 3 discrepancy cases, EM established a definitive diagnosis of metastatic colonic adenocarcinoma, and the two other cases EM diagnostic accuracy was limited by failure to obtain adequate sample. The following unique ultrastructural features in diagnosing 64 HCC cases were identified as: 1) Capillarization which were trabecular neoplastic hepatocytes surrounded by fenestrated or not separated endothelia with continuous basal lamina (Fig.1A); 2)altered bile canaliculi which commonly formed by more than three neoplastic hepatocytes and usually contained bile material (Fig.1B); 3) high atypical round to irregular shape nuclei with very large, ropy nucleoli that had nucleolonema (Fig.1C). Intranuclear cytoplasmic inclusions and giant mitochondria were also observed in the neoplastic cells.

Conclusions: Our results indicate that HCC displays unique ultrastructural features, which can be used as a reliable and accurate diagnostic tool for HCC in limited FNAC. EM is superior to FNAC in determining the tumor origin and in making more definitive diagnosis.

1950 "Cilia Metaplasia" in Renal Transplant Biopsies with Acute Tubular Injury.
HS Desai, JP Roszka, ML Kaiser, KL Dundas, MT Rooney, PL Zhang. William Beaumont Hospital, Royal Oak, MI.

Background: Primary cilia are hair-like organelles singly distributed along the apical surface of proximal and distal nephron tubules. They are known to play a mechanosensation role in tubular differentiation. A recent study demonstrated increased length of cilia in renal transplantation with acute tubular injury (ATI), using immunofluorescent method against alpha-tubulin, as an indicator of injury and repair (J Am Soc Nephrol 2009: 20: 2147-2153). In our study we used electron microscopy (EM) to evaluate cilia changes in acute tubular injury (ATI) in both transplant and native biopsies.

Design: Three groups of cases were included: control group 1- native biopsies without major changes in renal tubules; study group 2- native biopsies with prominent ATI, and study group 3- renal transplant biopsies with prominent ATI (delayed renal function group). Extensive search for ciliary structures along renal tubules (at least 10 15 fields at 6,500 magnification) was conducted in each case. When cilia were identified, high magnification (up to 130,000) was used to obtain images for detailed ultrastructural study. The search for cilia was focused on proximal tubular areas with injured (diminished) apical microvilli.

Results: Singly located cilia were found in 3/19 specimens in control group 1, 4/18 in group 2 (native ATI), and 6/24 in group 3 (transplant ATI). Importantly, there were clusters of cilia in proximal tubules with markedly diminished apical microvilli in 3/25 biopsies from two patients in group 3, but none from groups 1 and 2. The clusters of cilia ranged from 6 to 15 individual cilia along the apical surface with diminished apical microvilli.